W.D. Phillips, *Laser cooling and trapping of neutral atoms*, in *Laser Manipulation of Atoms and Ions*, edited by E. Arimondo, W.D. Phillips, and F. Strumia, Proceedings of the International School of Physics "Enrico Fermi", Course CXVIII (North-Holland, Amsterdam, 1992) pp. 289

Laser Cooling and Trapping of Neutral Atoms.

W. D. PHILLIPS

Atomic Physics Division, PHYS A167
National Institute of Standards and Technology
U. S. Department of Commerce, Technology Administration
Gathersburg, MD 20899

1. – Introduction.

These notes cover three lectures given at the Enrico Fermi Summer School on Laser Manipulation of Atoms and Ions, held in Varenna in July 1991. These three lectures have by no means covered the subject matter of laser cooling and trapping of neutral atoms, but, together with the other lectures given at the school on the subject, may be a useful introduction. The reader is also referred to the relevant notes for the Les Houches Summer School on Quantum Optics held in June and July of 1990 [1].

Subjects covered by these notes include: laser deceleration and cooling of atomic beams; the theory of the cooling limit and of optical molasses from the Doppler-cooling viewpoint; experiments with optical molasses in three dimensions, and the discovery of cooling below the Doppler-cooling limit; comparison of the experimental results with the theory of the new cooling mechanisms; trapping of atoms using the radiation pressure and dipole forces; applications of cooling and trapping to measurements of collisions and of the spectrum of resonance fluorescence.

For convenience and clarity, a number of repeatedly used symbols are defined here. All frequencies are expressed as angular frequencies, having units of radians/second. The reader is warned that other authors have used different conventions:

$\delta = \omega_{\text{laser}} - \omega_{\text{atom}}$ is the detuning of the laser frequency from the natural resonant frequency of the atom.

$\Gamma = \tau^{-1}$ is the decay rate of the population in the excited state, the inverse of the natural lifetime.

$k = 2\pi/\lambda = 1/\lambda$ is the photon laser wave vector.

Ω is the on-resonance Rabi frequency, the precession frequency of the Bloch vector with zero detuning and no relaxation.

$I/I_0 = 2\Omega^2/\Gamma^2$ is the normalized intensity of the laser. When there are multiple laser beams, this will generally refer to the intensity of a single beam.

M is the atomic mass.

$v_{rec} = \hbar k/M$ is the velocity with which the atom recoils upon emission or absorption of a single photon.

$E_{rec} = Mv_{rec}^2/2 = \hbar^2 k^2/2M$ is the kinetic energy of an atom having velocity v_{rec}.

2. – Deceleration and cooling of atomic beams.

Deceleration of an atomic beam is usually accomplished by directing a near resonant laser beam so as to oppose the atomic beam. The atoms absorb photons at a rate determined by the intensity of the laser beam, the detuning from resonance and the atoms' velocity. For each photon absorbed, the atomic velocity changes by v_{rec} in the direction of the laser propagation. The spontaneously emitted photons are emitted randomly in a pattern that is symmetric on reflection through the atom, so there is no net average change in the atomic velocity due to these emissions. If absorption is followed by stimulated emission into the same direction as the incident laser beam (we assume the laser beam is a plane wave), there is no net momentum transfer from the absorption-emission process. Only absorption followed by spontaneous emission contributes to the average force, which is given by the rate of scattering photons times the momentum of a photon. For a two-level atom this is

$$F = \hbar k \frac{\Gamma}{2} \frac{I/I_0}{1 + I/I_0 + \left[\frac{2(\delta - \boldsymbol{k}\cdot\boldsymbol{v})}{\Gamma}\right]^2} \tag{1}$$

In writing such a force we make the implicit assumption that the velocity does not change very much in the course of absorbing a few photons, *i.e.* $kv_{rec} \ll \Gamma$. This ensures that it is meaningful to speak of an «average» force (averaged over several absorption-emission events) for a given velocity.

Because only processes involving spontaneous emission contribute, the force (1) is often called the spontaneous force. It is also referred to as the radiation pressure force or scattering force. It is the velocity dependence of this force which leads to Doppler cooling. At high intensity this force saturates to the value $\hbar k\Gamma/2$. The spontaneous force is limited by the rate at which spontaneous emissions can occur. These occur at a rate Γ for excited atoms, whose maximum fractional population is $1/2$.

The acceleration of an atom due to the saturated radiation pressure force is $a_{max} = \hbar k\Gamma/2M = v_{rec}\Gamma/2$, which can be quite large. For sodium with $\lambda = 2\pi/k = 589$ nm, $1/\Gamma = 16$ ns and $M = 23$ a.m.u., $v_{rec} \approx 3$ cm/s and $a_{max} \approx 10^6\,\mathrm{m/s^2}$. For cesium, with $\lambda = 852$ nm, $1/\Gamma = 30$ ns and $M = 133$ a.m.u., $v_{rec} \approx 3.5$ mm/s and $a_{max} \approx 6 \cdot 10^4\,\mathrm{m/s^2}$. This acceleration would stop a thermal, 1000 m/s Na atom in 1 ms over 0.5 m, and a thermal, 300 m/s Cs atom in 5 ms over 80 cm.

For real, multilevel atoms the situation can be more complicated. A common occurrence, typical of alkali atoms, is that the ground state is split by the hyperfine interaction into two states separated by many times the optical linewidth Γ. An atom excited by a laser from one of these hyperfine levels to an optically excited state may decay by spontaneous emission to the other hyperfine level. Transitions from this level are then so far out of resonance that effectively no further absorption occurs and no force is applied to the atom. While various schemes involving selection rules and polarization of the light may be used to avoid this problem of optical pumping, the most straightforward method is to apply a second laser frequency, tuned to resonance between the «wrong» hyperfine state and the optically excited state. This «repumper» keeps the atom out of the wrong ground state and allows the atom to be effectively decelerated.

Another impediment to effective deceleration of an atomic beam is already implicit in (1). The force on an atom is only large if $|2(\delta - \boldsymbol{k}\cdot\boldsymbol{v})| \lesssim \Gamma\sqrt{1 + I/I_0}$. Atoms much outside this resonant-velocity range will experience little deceleration, and atoms initially within this range will be decelerated out of it. This process results in a cooling or velocity compression of a portion of the atomic beam's velocity distribution, and was first observed by ANDREEV *et al.* [2]. Atoms initially at the resonant velocity decelerate out of resonance. Other atoms with nearby velocities will also decelerate, those with larger velocities first decelerating into resonance, then to slower velocities out of resonance, while initially slower atoms decelerate to still lower velocities. The atoms will «pile up» at a velocity somewhat lower than the resonant velocity. Both deceleration and cooling occur because a range of velocities around the resonant velocity are compressed into a narrower range at lower velocity. The change in the velocity distribution of an atomic beam with a thermal spread of velocities is illustrated in fig. 1.

The difficulty with the velocity distribution of fig. 1 is that only a small portion of the total velocity distribution has been decelerated by only a small amount. There are a number of possible solutions to this problem, some of which have been discussed in [3]. These include Zeeman tuning [4] where a spatially varying magnetic field compensates the changing Doppler shift as the atoms decelerate so as to keep the atoms near resonance; white-light deceleration [5] where a range of laser frequencies ensures that some light is resonant with the atoms, regardless of their velocity (within the range to be decelerated); diffuse-light deceleration [6] where light impinges on the atoms from all

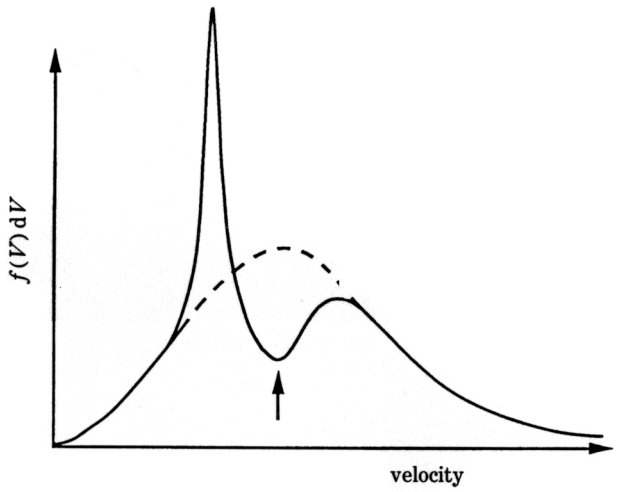

Fig. 1. – Longitudinal velocity distribution of an atomic beam before (dashed line) and after (full line) interacting with a counterpropagating, fixed-frequency laser. The arrow indicates the velocity resonant with the laser.

angles so that, with the Doppler shift, some of the light is resonant with each velocity. Here we discuss «chirp cooling» in which the frequency of the laser is swept up, or chirped, in time [7]. Because of the chirp, atoms that have been decelerated by the laser stay in resonance, continue to absorb photons, and continue to decelerate. Furthermore, the chirp brings the laser into resonance with additional atoms having lower velocities than the original group around the velocity initially resonant with the laser.

In order to analyze this process, let us consider atoms having positive velocities near some velocity V opposed by a laser beam propagating in the negative direction. We express any atomic velocity as $v = V + v'$. The acceleration of atoms having velocity V ($v' = 0$) is $a = F(V)/M$, where $F(V)$ is given by (1). Therefore, we write $V(t) = V(0) + at$. Also we let the detuning vary as $\delta(t) = \delta' - kV(t)$. That is, we chirp the laser frequency so as to stay a constant detuning δ' from resonance with atoms having the decelerating velocity $V(t)$. Now we transform to a frame decelerating with $V(t)$. In this frame the atomic velocity is v' and the laser detuning is Doppler shifted to δ'. The force on an atom in this frame is

$$F(v') = \hbar k \frac{\Gamma}{2}\left[\frac{-I/I_0}{\left[\frac{2(\delta' + kv')}{\Gamma}\right]^2} + \frac{I/I_0}{1 + I/I_0 + \left[\frac{2\delta'}{\Gamma}\right]^2}\right] \tag{2}$$

The minus sign of the first term in large brackets comes from the laser propagating in the negative direction. The second term in the large brackets is the «fictitious» inertial force felt by an atom in the decelerating frame. Expanding this expression for small v', we get

$$F(v') = 2\hbar k^2 \frac{I}{I_0} \frac{(2\delta'/\Gamma)v'}{\left[1 + I/I_0 + \left(\frac{2\delta'}{\Gamma}\right)^2\right]^2}. \tag{3}$$

The term multiplying v' is minus the friction coefficient α. When $\delta' < 0$, the force opposes the velocity v' and tends to damp all velocities to zero in the decelerating frame, which is $V(t)$ in the laboratory frame. Maximum damping occurs for $I/I_0 = 2$ and $2\delta'/\Gamma = -1$. The final velocity to which the atoms are decelerated is determined in practice by the final frequency to which the laser is chirped. Figure 2 shows the results of chirp cooling an atomic beam. All of the atoms in the initial distribution below the velocity resonant with the laser at the beginning of its chirp are decelerated.

The first definitive experiment showing such chirp cooling was in ref. [8], with deceleration to zero velocity first achieved in ref. [9]. The analysis given above is similar to that given in ref. [10].

The robust character of this sort of cooling is evident. Atoms within a range of velocities around $V(t)$ are damped (in velocity) toward $V(t)$. Lower velocities, not initially close to $V(t)$, come within range as the laser chirp brings $V(t)$ into

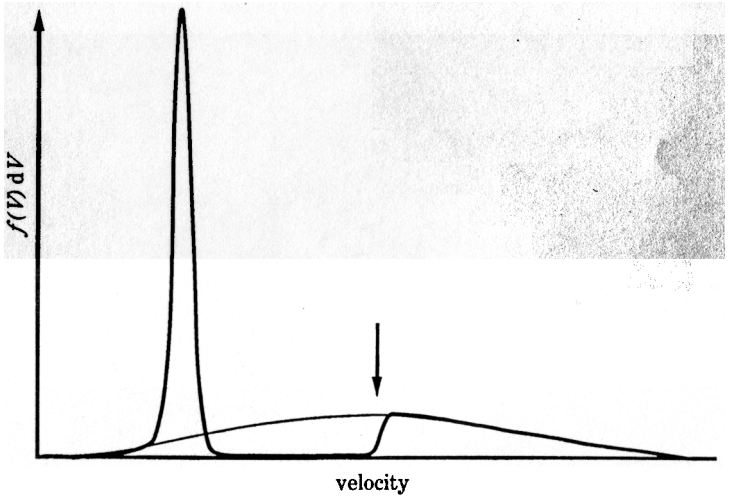

Fig. 2. – Longitudinal velocity distribution of an atomic beam before (thin line) and after (bold line) deceleration by a chirped laser. The arrow indicates the velocity initially resonant with the laser.

coincidence with them. If the laser intensity changes during the time an atom is being decelerated (because, for example, the laser beam is not collimated), the atoms will continue to decelerate according to the chosen chirp rate, but with a different effective detuning δ'. That chosen chirp rate, however, must be consistent with an achievable deceleration with the given I/I_0. That is, the chirp rate must satisfy

$$\dot{\delta} = ka = \frac{\hbar k^2 \Gamma}{2M} \frac{I/I_0}{1 + I/I_0 + \left[\frac{2\delta'}{\Gamma}\right]^2}. \tag{4}$$

This means that $\dot{\delta}$ has an allowable upper limit of $ka_{\max}$. We have noted that for the velocities to be damped in the decelerating frame we must have $\delta' < 0$ and it is easy to show that the conditions for best damping lead to a deceleration half as large as the maximum.

3. – The Doppler-cooling limit.

So far we have considered only the time average of the radiation pressure force (1). In the one-dimensional case of chirp cooling viewed in the decelerating frame, this leads to the friction force (3). Writing this force as $F = -\alpha v$ (dropping the primes) we conclude that the atom loses kinetic energy at a rate $\dot{E}_{\text{cool}} = Fv = -\alpha v^2$. The energy damps to zero at a rate $\dot{E}/E = -2\alpha/M$. The radiation pressure that produces the damping force results from discrete transfers of momentum when the atom absorbs or emits photons. This discreteness means that the force fluctuates about the average value. The fluctuations tend to heat the atom. To visualize this heating, assume that the average force is zero (as when $v = 0$), but the atom is subject to a fluctuating force of zero mean arising from the absorptions and emissions. Each event transfers momentum to the atom, and, in the limit of low intensity, each event is uncorrelated with other events, transferring momentum in a random direction, at a random time. The randomness is a direct consequence of the random character of spontaneous emission. As a result, the atomic momentum undergoes a random walk. The mean square of the momentum increases with time, which is to say the kinetic energy increases, and the atom heats. This diffusion of the atomic momentum has been treated in detail by a number of authors [11-13]. Here we will follow a simple calculation for weak fields.

Let us calculate the rate of heating in a «ideal» one-dimensional situation, a two-level atom in a weak wave traveling along the x-axis, with the spontaneous photons assumed to be emitted only along this axis. There are two contributions to the heating: the random direction of the spontaneous emissions and the randomness of the absorption. Each spontaneously emitted photon goes in a direction which is uncorrelated with that of other emitted photons, so these emissions induce a random walk with momentum step size $\hbar k$. After N emissions, according to the usual random-walk theory, the mean square momentum is $\langle p_x^2 \rangle = N\hbar^2 k^2$. The momentum diffusion coefficient is defined in terms of the rate of increase of $\langle p^2 \rangle$, which in turn depends on the rate of emitting photons:

$$2D_{\text{spont}} = \langle \dot{p}_x^2 \rangle = \hbar^2 k^2 \frac{\Gamma}{2} \frac{I/I_0}{1 + I/I_0 + (2\delta/\Gamma)^2}. \tag{5}$$

For low intensity, successive absorptions are uncorrelated (we are assuming that kv, $kv_{\text{rec}} \ll \Gamma$, and the Doppler shift due to a recoil velocity does not much change the relative absorption probability), so the number of photons absorbed in any time interval is distributed according to Poisson statistics. The variance in the number absorbed for a Poisson distribution is equal to the mean number absorbed (which is also the mean number emitted), so the absorption contribution to the momentum diffusion $D_{\text{abs}} = D_{\text{spont}}$. (This equality holds only as long as the intensity is low. In a high-intensity field the absorption statistics can be non-Poissonian, so that variance in the number of absorbed photons in a given time is not equal to the average number. In that case we will have $D_{\text{abs}} = D_{\text{spont}}(1 + Q)$, where Q is Mandel's parameter describing the non-Poissonian character. The non-Poissonian character is discussed in more detail in ref. [11, 13]. For most situations involving Doppler cooling, Q will be small and we will ignore it in what follows.)

Now we equate the rate of increase of kinetic energy due to the diffusion (from both absorption and spontaneous emission) to the rate of decrease in kinetic energy due to the damping of friction. Thus, in steady state,

$$\langle \dot{E}_{\text{heat}} \rangle = \frac{\langle \dot{p}^2 \rangle}{2M} = \frac{D}{M} = -\langle \dot{E}_{\text{cool}} \rangle = \alpha \langle v^2 \rangle, \tag{6}$$

where D is the total diffusion coefficient, $D_{\text{spont}} + D_{\text{abs}}$. For this 1-D problem we have a single degree of freedom, so $M\langle v^2 \rangle/2 = k_B T/2$. This temperature is

$$k_B T = \frac{D}{\alpha} = -\frac{\hbar\Gamma}{4} \frac{1 + I/I_0 + \left(\frac{2\delta}{\Gamma}\right)^2}{\frac{2\delta}{\Gamma}} \tag{7}$$

If the intensity is low, this can be written as

$$k_B T = -\frac{\hbar\Gamma}{4}\left(\frac{\Gamma}{2\delta} + \frac{2\delta}{\Gamma}\right). \tag{8}$$

This expression is plotted in fig. 3. This illustrates why the detuning should not be too small (or too large), since small detunings lead to high temperatures.

In this low-intensity limit the temperature minimizes for $\delta = -\Gamma/2$, giving

$$k_B T_{\text{Dop}} = \frac{\hbar\Gamma}{2}, \tag{9}$$

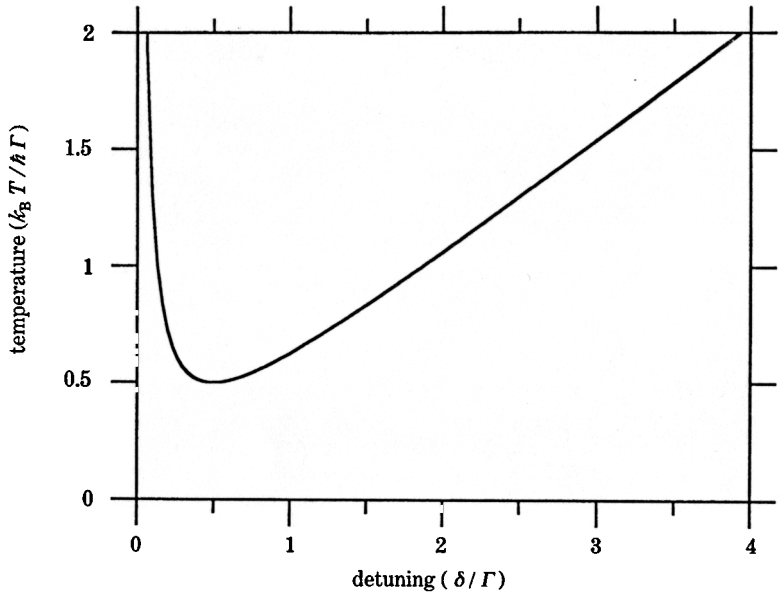

Fig. 3. – Equilibrium temperature for laser cooling at low intensity as a function of laser detuning.

where T_{Dop} is called the Doppler-cooling limit. Note that this limit is different from ones often given for Doppler cooling in 1-D. In some other treatments the spontaneous emission is not assumed to be along the 1-D axis, but distributed in a manner characteristic of an isotropic, dipole, or other radiation pattern. With such an assumption, which would be appropriate for a «real» 1-D situation such as collimation of an atomic beam along one direction, the 1-D temperature is smaller than in eq. (8). The actual value will depend on the nature of the radiation pattern. The Doppler limit for our idealized 1-D case corresponds to 240 μK, a 1-D r.m.s. velocity of 30 cm/s for sodium and 125 μK and 9 cm/s for cesium.

An atom undergoing chirp cooling by a single traveling wave has the same Doppler-cooling limit (viewed in the decelerating frame) as does an atom in weak counterpropagating beams, as we shall see below.

4. – Optical molasses in one dimension.

In the treatment of deceleration given above, we transformed into an accelerating frame where the radiation pressure force was opposed and compensated by an inertial force in that frame. The total force on zero-velocity atoms in the chosen frame is zero (eqs. (2), (3)), and negative detuning makes this velocity a

point of stable equilibrium. If we wish to have the same situation in the laboratory rest frame, we must have a real force to compensate the radiation pressure. This force might be provided by an electric field if the atoms are charged [14], or, more generally, by an opposing radiation pressure.

A configuration of counterpropagating laser beams used for cooling of atoms has come to be known as «optical molasses» [15]. This is the situation envisaged by HÄNSCH and SCHAWLOW [16] in their 1975 proposal for laser cooling. The contemporary proposal by WINELAND and DEHMELT [17] contains the same essential idea, developed in such a way as to be more relevant to the laser cooling of trapped ions.

If the intensity of each beam is small ($I/I_0 \ll 1$), we can write the total force on an atom as the sum of the radiation pressure from each of the two beams, as long as we understand this to be the force averaged over a wavelength of the light. In one dimension:

$$F(v) = \hbar k \frac{\Gamma}{2} \frac{I/I_0}{1 + \left[\frac{2(\delta - kv)}{\Gamma}\right]^2} - \hbar k \frac{\Gamma}{2} \frac{I/I_0}{1 + \left[\frac{2(\delta + kv)}{\Gamma}\right]^2}. \tag{10}$$

Figure 4 shows the force from each of the beams (solid curves) and the total force (dashed curves) for a variety of detunings.

This series of plots illustrates the fact that the slope of $F(v)$ at $v = 0$ has a maximum near $2\delta/\Gamma = -1$. Furthermore, $F(v)$ is linear only over a range of velocities on the order of Γ/k. For small v and I/I_0 the force is given by

$$F(v) = 2\hbar k^2 \frac{(2I/I_0)(2\delta/\Gamma)v}{\left[1 + \left(\frac{2\delta}{\Gamma}\right)^2\right]^2} = -\alpha v. \tag{11}$$

The friction coefficient $\alpha = \gamma M$. The characteristic time for damping the atomic velocity is γ^{-1}. For a given, small value of I/I_0 the damping time is minimized for $2\delta/\Gamma = 1/\sqrt{3}$. Near this detuning, $\tau_{damp} \equiv \gamma^{-1} \approx T_{ext}(I/I_0)$, where $T_{ext} = \hbar/E_{rec}$ is the external time scale. Note that if the saturation parameter

$$s = \frac{I/I_0}{1 + \left(\frac{2\delta}{\Gamma}\right)^2} \tag{12}$$

is held constant (and small), the friction and thus the damping rate are maximized at $2\delta/\Gamma = 1$.

For $I/I_0 \ll 1$, eq. (3), derived for cooling with a single traveling wave, is identical to eq. (11) except that in (11) I/I_0 has been replaced with $2I/I_0$. Furthermore, for the weak-standing-wave case, the diffusion constant is just twice what it is for the weak traveling wave. In both cases, it is the presence of two beams, each of intensity I/I_0, which accounts for the factor of two. Since the

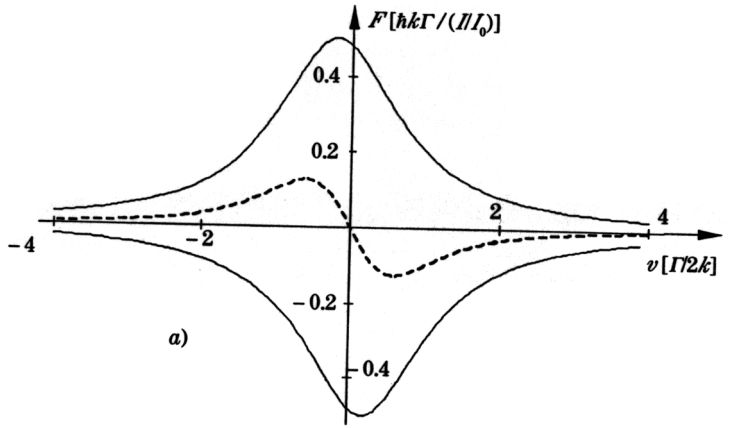

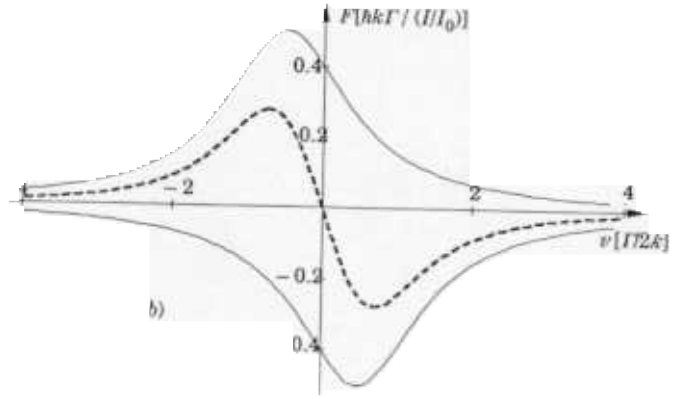

Fig. 4. – Weak-standing-wave radiation pressure force (in units of $\hbar k\Gamma/(I/I_0)$) *vs.* velocity (in units of $\Gamma/2k$) for various values of the detuning: *a*) $2\delta/\Gamma = 0.2$, *b*) $2\delta/\Gamma = 0.5$, *c*) $2\delta/\Gamma = 1$, *d*) $2\delta/\Gamma = 2$, *e*) $2\delta/\Gamma = 4$.

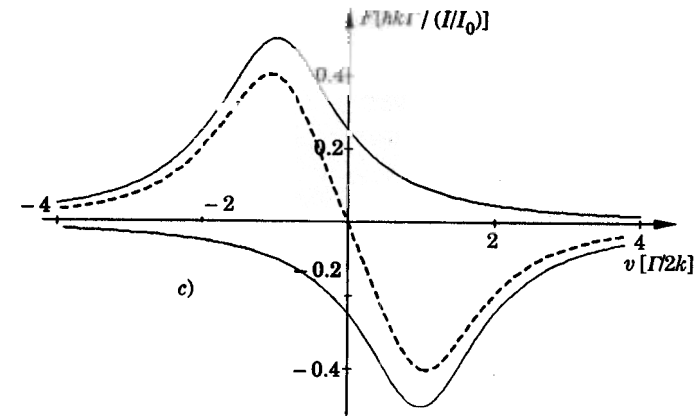

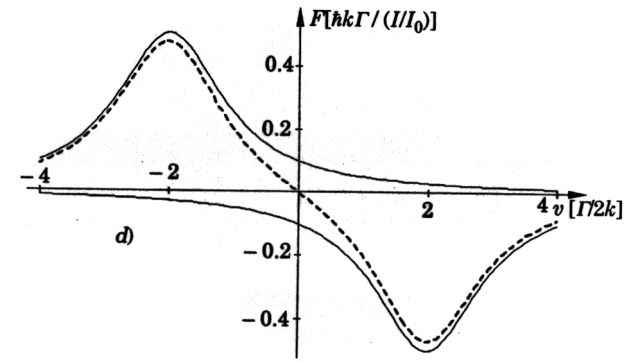

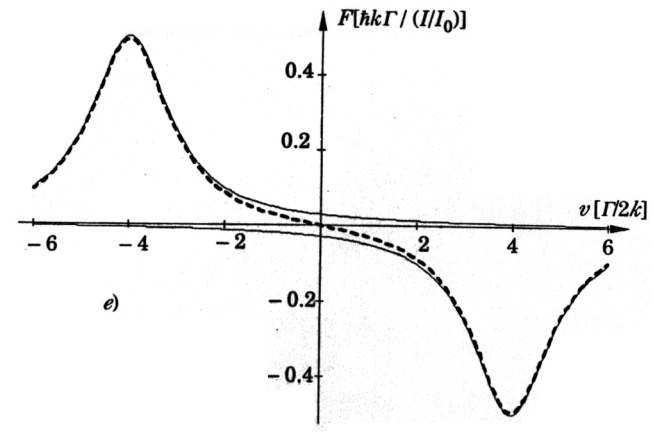

Fig. 4 (*continued*).

temperature is proportional to the ratio of diffusion to damping, the temperature in a weak 1-D molasses is identical to that in a weak traveling wave. There has been some confusion on this point because of the way in which D_{abs} is considered. We have considered it as arising from the fluctuations in the number of absorbed photons in a given time interval. In a standing wave, when one takes account of the variation of intensity along the standing wave, it may also be thought of as a fluctuation of the stimulated or dipole force [11]. (See also the discussion of this point in subsect. 10·2 in these notes.) In the absence of a standing wave, it might appear that, since there is no dipole force, there is no fluctuation of that force, so the momentum diffusion and the Doppler temperature should be less. In fact, as we have seen above, this is not so, and this term in the diffusion still exists in the case of a traveling wave.

In the above treatment, we have consistently taken $I/I_0 \ll 1$ in 1-D. This allowed us to treat the standing wave as the sum of two traveling waves. There are treatments of the high-intensity standing-wave case in 1-D for a 2-level atom (see, for example, [11-13]), and for the $J = 0 \to J = 1$ transition [18]. Unfortunately, these treatments do not easily generalize to the 3-D case we wish to treat later. We do have an exact treatment for a single, traveling, plane wave at arbitrary intensity, exemplified by eqs. (1)-(3). Using this result we can model strong counterpropagating waves as alternating traveling waves. This model was developed by DALIBARD [12] and is similar to one given by STENHOLM at this Summer School.

Consider two opposed running waves, alternated in time, with 50% duty factor. The average intensity of each wave is I, while the peak intensity is $2I$. We also assume that the time T for which each wave is on is such that $\gamma^{-1} \gg T \gg \Gamma^{-1}$, recalling that γ and Γ are the cooling rate and the natural decay rate, respectively. Since there is only one wave on at a time, and the transient time Γ^{-1} is negligible compared to T, we can simply add the forces from each wave to obtain the total average force:

$$\langle F \rangle = \hbar k \frac{\Gamma}{2} \left[\frac{1}{2} \frac{2I/I_0}{1 + 2I/I_0 + \left[\frac{2(\delta - kv)}{\Gamma} \right]^2} - \frac{1}{2} \frac{2I/I_0}{1 + 2I/I_0 + \left[\frac{2(\delta + kv)}{\Gamma} \right]^2} \right]. \tag{13}$$

The factor of $1/2$ before each term is from the duty factor, while $2I$ is the instantaneous intensity. Note that the term $2I/I_0$ in the denominators looks as if it is due to saturation and power broadening from the average power summed over both waves, although it is, of course, due to the instantaneous intensity of a single wave.

As before, we find the friction coefficient:

$$\gamma M = \alpha = -4\hbar k^2 \frac{I}{I_0} \frac{2\delta/\Gamma}{\left[1 + \frac{2I}{I_0} + \left(\frac{2\delta}{\Gamma} \right)^2 \right]^2}. \tag{14}$$

This is the same friction coefficient seen in eq. (11), except for the «saturation» factor in the denominator.

We may take this expression for the friction coefficient as exact for the alternated-wave case, or as an approximation for the case of continuous counterpropagating waves each of intensity I. The approximation ignores effects due to the standing-wave character of the counterpropagating waves. These are treated in, for example, [11-13]. Nevertheless, it is a fair approximation for $I/I_0 \lesssim 1$. An analysis in ref. [19] compares this model to the exact solutions for a 2-level system [11-13] and for the case of counterpropagating waves of opposite circular polarization ($\sigma^+ - \sigma^-$) on a $J = 0 \to J = 1$ transition [18]. The model agrees moderately well with the $\sigma^+ - \sigma^-$ calculation even for large intensity (and, accidentally, agrees exactly for $I/I_0 = 4$). The model disagrees dramatically from the 2-level calculation when $I/I_0 > 1$. This is because the model admits no possibility of absorption from one wave followed by stimulated emission induced by the other. This process does not occur in the $\sigma^+ - \sigma^-$ case, but dominates the behavior of a 2-level atom in a standing wave of high intensity.

Now consider the momentum diffusion coefficient in our alternated-wave model. In analogy with eq. (5) we can write the spontaneous part of the diffusion as

$$2D_{spont} = \langle \dot{p}_x^2 \rangle = \hbar^2 k^2 \frac{\Gamma}{2} \frac{2I/I_0}{1 + 2I/I_0 + (2\delta/\Gamma)^2}. \tag{15}$$

Because of the non-Poissonian nature of the absorption statistics at nonnegligible intensity, the part of the diffusion ascribed to the absorption is not the same as that for the spontaneous emission. Assuming as always that the emissions are all along the 1-D axis, we have $D_{abs} = D_{spont}(1 + Q)$. Thus the total diffusion $D = D_{spont}(2 + Q)$. For the intensities where the alternating model is a good approximation to a standing wave, $Q \ll 2$, so we will neglect it for the following discussion [13].

5. – Optical molasses in N dimensions.

This alternated-beam model easily generalizes to 2 or 3 dimensions, where we assume a $2N$-fold alternation where N is the dimension (each beam has intensity $2NI$ for $1/2N$ of the time). Then for the friction coefficient along any of the N axes we have

$$\gamma M = \alpha = -4\hbar k^2 \frac{I}{I_0} \frac{2\delta/\Gamma}{\left[1 + \frac{2NI}{I_0} + \left(\frac{2\delta}{\Gamma} \right)^2 \right]^2}, \tag{16}$$

and the total diffusion constant, the sum of the diffusion constants along each

axis, is

$$D = 2D_{\text{spont}} = \hbar^2 k^2 \frac{\Gamma}{2} \frac{2NI/I_0}{1 + 2NI/I_0 + (2\delta/\Gamma)^2} \tag{17}$$

We will use these expressions to obtain approximate results, for moderate intensity, in 3-D optical molasses.

(Note that in eq. (17) the momentum diffusion coefficient has been presented as a scalar. In actuality, it is a tensor given by $2D_{ij} = \langle \dot{p_i} p_j \rangle$. For the alternating-beam model, there is no correlation between photon scattering from the various beams, so the tensor is diagonal. Furthermore, for a 3-D symmetric situation such as isotropic photon scattering, or dipole scattering induced by three pairs of beams with mutually orthogonal linear polarization, or for our assumption that all spontaneous emissions are along the laser beam axis, the diagonal elements of the diffusion tensor are equal and the same for each case, so we may treat the diffusion as a scalar.)

For this case where all the axes of the N-D molasses are equivalent, we can write the friction force as $\boldsymbol{F} = -\alpha \boldsymbol{v}$. Then, as in 1-D, $\langle \dot{E}_{\text{heat}} \rangle = D/M$ and $\langle \dot{E}_{\text{cool}} \rangle = -\alpha \langle v^2 \rangle$. From the equipartition theorem we have $N k_B T/2 = \sum_{i=1}^{N} M \langle v_i^2 \rangle/2 = M \langle v^2 \rangle/2$, so the equilibrium temperature is given by

$$k_B T = \frac{D}{N\alpha} = \frac{\hbar\Gamma}{4} \frac{1 + \frac{2NI}{I_0} + \left(\frac{2\delta}{\Gamma}\right)^2}{\frac{2\delta}{\Gamma}} . \tag{18}$$

For low intensity this reduces to eq. (8), the temperature in 1-D.

We can maximize the friction coefficient given in eq. (16) with respect to both intensity and detuning, finding

$$\gamma M = \alpha = \frac{\hbar k^2}{4N} \quad \text{for } 2\delta/\Gamma = -1 \text{ and } I/I_0 = 1/N. \tag{19}$$

For sodium in this approximation the minimum damping time is $\gamma^{-1} = 13\ \mu\text{s}$ in 1-D and 40 μs in 3-D. For cesium the times are 160 μs and 480 μs, respectively. The reduced damping in 3-D is due to the duty factor in the alternated-beam model. If we consider this as a model of continuous 3-D molasses, then we may interpret the reduction as being due to the fact that an atom moving along any given axis spends 2/3 of its time interacting with beams perpendicular to its velocity.

With the parameters of eq. (19), eq. (18) gives $k_B T = \hbar\Gamma$ (independent of the number of dimensions), just twice the Doppler-cooling limit. In the low-intensity limit the minimum temperature is achieved for the same conditions as in 1-D, and is the same as the 1-D limit. (This equality depends on our having assumed that the spontaneous emissions in 1-D are all along the 1-D axis.) For either

maximum friction or minimum temperature, an atom in N-D has N times as much kinetic energy as in 1-D, but the same energy per degree of freedom, which is to say the same temperature.

We may inquire whether the atoms truly have a temperature. This is a rather subtle question, but we can say that, if the damping force is linear in velocity and if the diffusion constant is independent of velocity, the solution of the Fokker-Planck equation describing the system yields a Maxwell-Boltzmann distribution of velocities. In reality, neither of these conditions is exactly fulfilled. Furthermore, the writing of a Fokker-Planck equation assumes that the discreteness of the velocity changes can be ignored. Fortunately, for most cases the conditions are sufficiently fulfilled that the distribution of velocities is expected to be very nearly thermal. For sodium atoms the equilibrium velocity distribution is generally well within the velocity regime where the force is linear in velocity and the diffusion is constant, justifying the assumption *a posteriori*. Also, we have assumed at the beginning that $k v_{\text{rec}} \ll \Gamma$, justifying the assumption that the discreteness of the force is small enough that a differential equation can be written. In ref. [19] a Monte Carlo simulation of optical molasses in sodium, including the effects of single-photon recoil and all the nonlinearities of the force and diffusion, produced a velocity distribution indistinguishable from a thermal one.

6. – Spatial diffusion in optical molasses.

We will apply the above model for 3-D molasses to study the atomic motion using a Brownian-motion approach. Let us estimate the distance an atom will diffuse in a time t_d. Moving at a thermal velocity $v_{\text{r.m.s.}}$ the atom will travel a distance $l = v_{\text{r.m.s.}}/\gamma$ during a damping time. Considering this l as a random-walk step which is repeated $t_d \gamma$ times, the mean square distance diffused in t_d is

$$\langle r^2 \rangle \approx l^2 t_d \gamma = \frac{D^p t_d}{\alpha^2} , \tag{20}$$

where D^p is the momentum diffusion coefficient. More rigorously, we can define a spatial diffusion constant D^x by $\langle x^2 \rangle = 2 t_d D^x$. A careful treatment (see ref. [15, 19] and references therein) gives $D^x = k_B T/\alpha$ and

$$\langle r^2 \rangle = \frac{2 D^p t_d}{\alpha^2} . \tag{21}$$

Using eqs. (16), (17) and maximizing the diffusion time in (21) for a given diffusion distance we find [19]

$$t_d^{\max} = \frac{4k^2 \langle r^2 \rangle}{27 N^2 \Gamma} \tag{22}$$

for $2\delta/\Gamma = -1$ and $I/I_0 = 1/2N$. The times to diffuse 0.5 cm in 3-D for sodium and cesium are 750 ms and 675 ms, respectively. If we assume the atoms diffuse to the edge of a spherical region (an approximation to the intersection region of three pairs of finite-cross-section laser beams) and then are lost, we find that the number of atoms within the sphere decays as the sum of exponentials [15, 19]. In 3-D the leading term decays with a time constant $t_M = 6t_d/\pi^2$. This is usually referred to as the molasses lifetime.

If an external force is applied to an atom in optical molasses, it will acquire drift velocity such that the friction force cancels the external force:

$$v_{drift} = F_{ext}/\alpha . \tag{23}$$

If the external force is gravity, we have $v_{drift} = g/\gamma$. For the maximum damping conditions of eq. (19) in 3-D, the gravity-induced drift is 0.4 mm/s for sodium and 5 mm/s for cesium. This would be quite a significant effect for a centimeter diameter cesium molasses, limiting the molasses lifetime to something on the order of a second. Another source of «external» force might be an imbalance in the intensity of counterpropagating beams. In ref. [19] an approximate treatment shows that for optimum damping conditions the drift velocity is given by $v_{drift} = \varepsilon\Gamma/2k$, where ε is the fractional imbalance. For sodium or cesium a 1% imbalance gives a drift of about 3 cm/s, a significant effect. In fact, as we shall see later, and as explained in [13], and in Cohen-Tannoudji's notes for this Summer School, experimental optical molasses for an atom such as cesium works quite differently from the simple description given here, appropriate for a 2-level atom. Experiments show that optical molasses is far more resistant to the effects of unbalanced forces than the calculations here imply.

7. – Experiments with optical molasses.

7·0. *Introduction.* – The first experiments with optical molasses were conducted against a background of the theory of Doppler cooling as outlined above. Soon it became clear that the observations on optical molasses were inconsistent with that theory. The mounting evidence of disagreement between theory and experiment culminated in the discovery that the temperature of atoms in optical molasses was much lower than the Doppler-cooling limit. This led to the identification of a new class of laser cooling mechanisms (treated extensively by COHEN-TANNOUDJI at this Summer School) which operate in multilevel systems where optical pumping and differential light shifts are possible. This section traces some of the experimental developments associated with this revolution in laser cooling.

7·1. *The early experiments.* – Optical molasses, as a medium for the quasi-confinement of atoms, was first conceived and observed by CHU and colleagues at Bell Labs in 1985 [15]. Using chirp cooling of a pulsed atomic sodium beam

they created atoms with velocities low enough to be captured by the molasses. The molasses was the classic 3-D configuration of three mutually orthogonal pairs of counterpropagating laser beams. By observing the fluorescence after the molasses is loaded with atoms they measured the molasses lifetime, the decay of the density of atoms due to spatial diffusion of atoms out of the laser beams. The observed lifetime on the order of 0.1 s was in good agreement with the expectation based on a calculation such as that of eq. (22).

The temperature was measured by a ballistic technique now known as «release and recapture». After the molasses is loaded and allowed to come to a quasi-equilibrium, and the density is slowly decaying with the molasses lifetime, the molasses lasers are abruptly switched off for a period of time t_{off}. With the confining lasers off, the atoms previously held by the viscous molasses forces are released to move freely and ballistically, feeling only the influence of gravity. During this ballistic period some atoms leave the volume in which they were initially confined. When the laser beams are turned back on, the atoms remaining in that volume are recaptured by the molasses. The ratio of the number of atoms in the molasses (as measured by the fluorescence) after the recapture to the number before the release gives information about how fast the atoms were traveling at the moment of release (see fig. 5). In practice the temperature is determined by comparing this ratio, as a function of the time the molasses is off, to the prediction for a given temperature. The result of the Bell Labs measurement was 240^{+200}_{-60} μK.

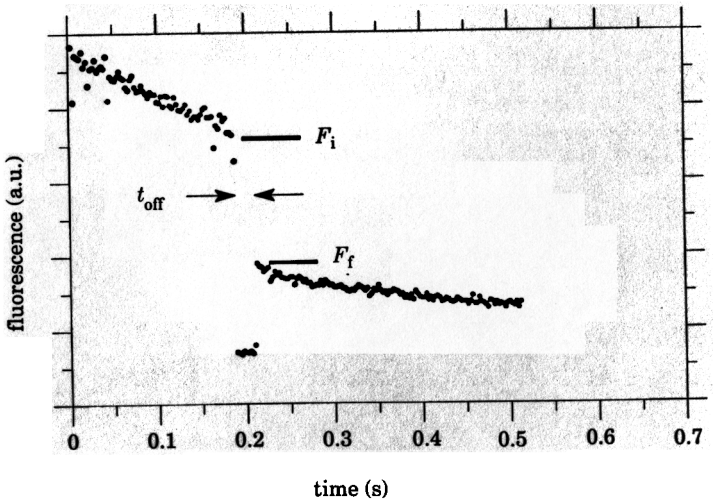

Fig. 5. – Fluorescence as a function of time for the release and recapture method of temperature measurement. The ratio of the fluorescence before (F_i) and after (F_f) the ballistic period t_{off} is used to determine the temperature.

The combination of a measured molasses lifetime in the expected range and a measured temperature equal to the expected Doppler-cooling limit was taken as satisfying verification that optical molasses was well understood. The fact that the Doppler limit was obtained, even though it is to be expected only in the limit of low intensity, was mildly disturbing. However, the uncertainty of the measurement, and the fact that during the release the laser beams were turned off slowly enough that the molasses temperature could have equilibrated to the low-intensity limit, made the results seem reasonable. Later measurements [20] of the temperature in an atomic cesium molasses also gave results near the Doppler-cooling limit.

Soon, some additional measurements raised questions about the apparent agreement of theory and experiment. The Bell Labs group reported a curious phenomenon they called «super molasses» [21] which occurred at high laser intensity. The super molasses had an anomalously long diffusion lifetime, and with laser intensity considerably greater than the predicted optimum intensity. The group at NIST also reported anomalous behavior [22]. In particular, the molasses lifetime plotted as a function of laser detuning (see fig. 6) had a very different dependence from that predicted by the theory outlined in sect. 6. In other measurements, the expected drift velocity (see eq. (23)) for a laser intensity imbalance was not seen [22]. These observations suggested that the theory of Doppler cooling was inadequate to explain the behavior of optical molasses.

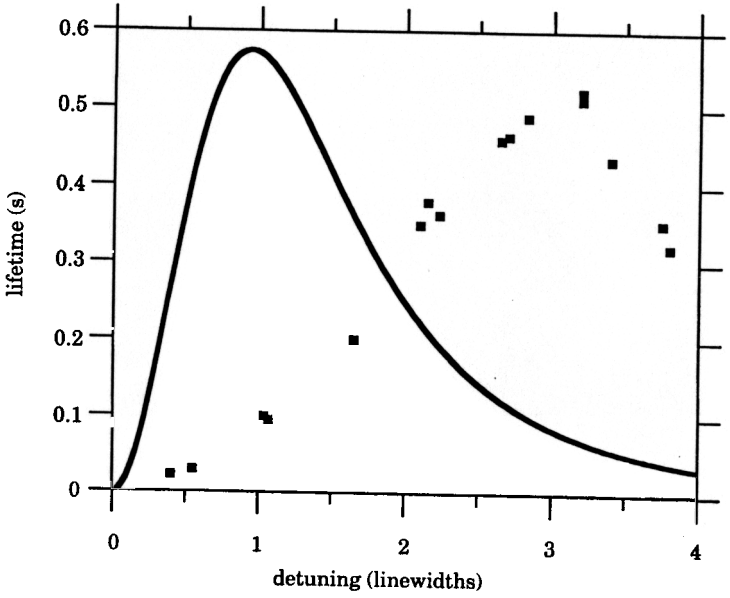

Fig. 6. – Predicted (curve) molasses lifetime for Doppler cooling with $I/I_0 = 0.5$, compared to measurements (points).

7·2. *Sub-Doppler temperatures.* – In an attempt to resolve the difficulties posed by results such as those of fig. 6, the NIST group decided to make more detailed and accurate temperature measurements [23]. The large uncertainty in the release and recapture technique is due to uncertainty in the distribution of

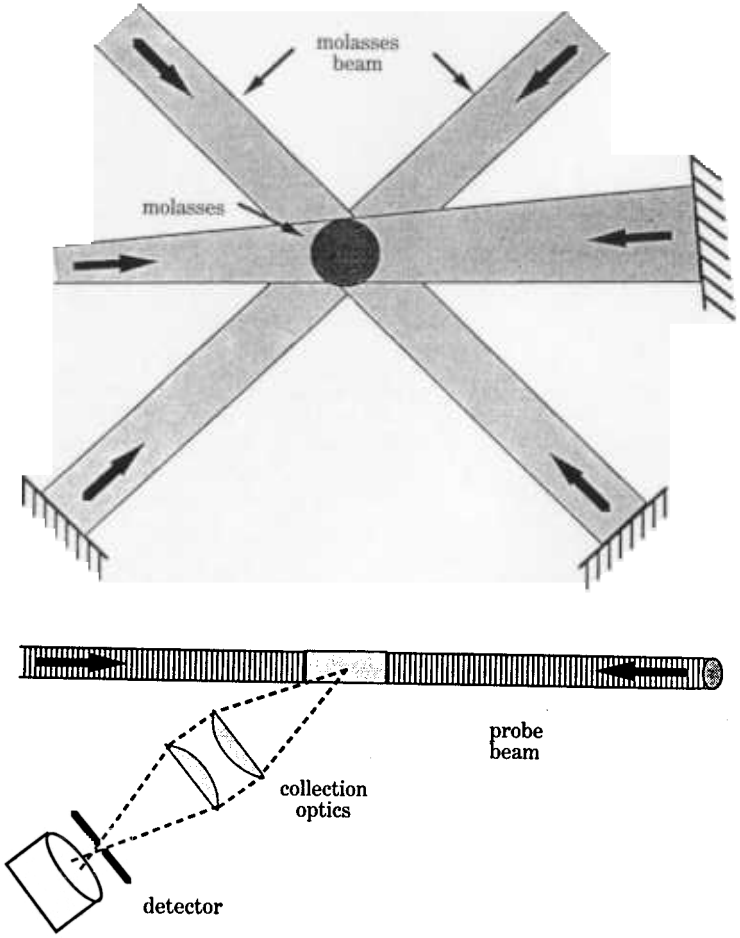

Fig. 7. – Time-of-flight technique of temperature measurement used at NIST. Atoms are released from the optical molasses and travel ballistically to the probe region.

atoms in the molasses before release, and to uncertainty in the capture volume of the molasses. This latter problem is made worse by any nonuniformity in the molasses laser beam intensities. To avoid such difficulties the NIST group used a time-of-flight (TOF) technique illustrated in fig. 7. As before, the molasses is loaded with slow atoms. Color Plate II is a photograph of such a molasses. (The NIST experiments loaded with a continuous atomic beam cooled by the Zeeman-tuned technique, rather than a pulsed, chirp-cooled beam as at Bell Labs, but this should have no effect on the subsequent molasses behavior.) After the loading is terminated and the molasses has equilibrated and begun to decay, the molasses beams are cut off, releasing the atoms. The arrival of the released atoms in a detection region separated from the molasses is observed by recording the fluorescence induced by the counterpropagating pair of laser beams forming the detection region. The distribution of arrival times (TOF spectrum) is compared to a calculated distribution to determine the temperature. If the probe separation from the molasses is large compared to the molasses radius, the details of geometry that limit the accuracy of the release and recapture method become unimportant.

The TOF measurements showed the temperature to be much lower than the Doppler-cooling limit. Figure 8 gives an example of one of the lower temperatures observed for sodium. The 25 μK is about a factor of ten lower than the

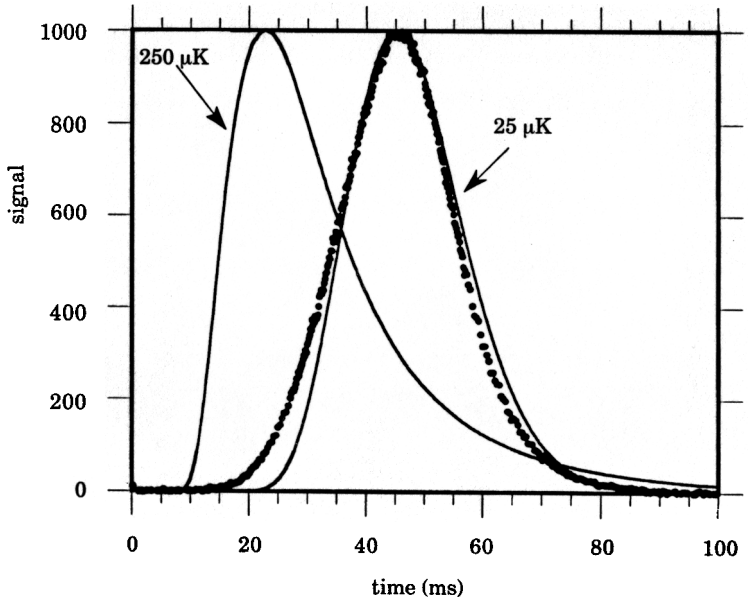

Fig. 8. – Time-of-flight spectrum for sodium atoms released from optical molasses. Calculated curves for 25 μK and 250 μK are shown.

Doppler-cooling limit. Even considering the uncertainty of about ± 15 μK associated with this measurement, the temperature is without question far below the Doppler temperature.

Additional measurements [19,23] showed that the temperature depended on the polarization of the molasses laser beams, that the temperature was a nearly monotonically decreasing function of detuning from resonance (see fig. 9), and

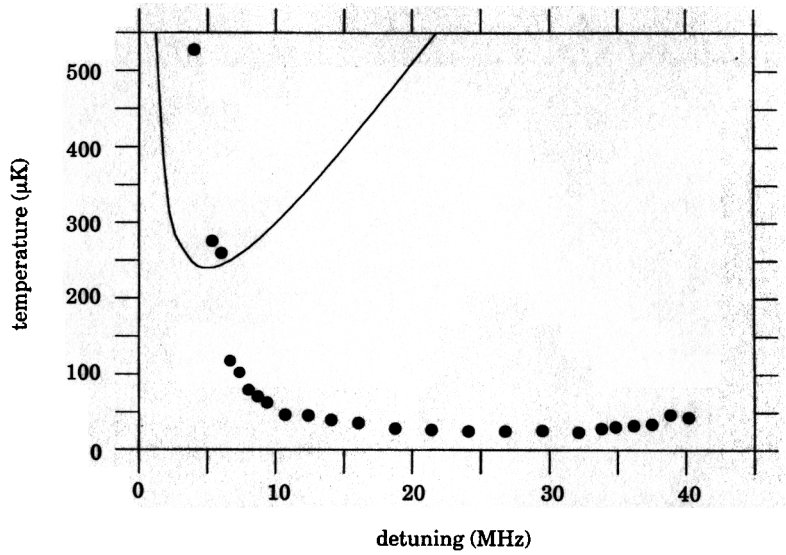

Fig. 9. – Temperature as a function of detuning for sodium atoms released from optical molasses (points) and Doppler temperature (curve).

that the temperature as well as the lifetime of the molasses were strongly dependent on magnetic field. All of this was inconsistent with the theory of Doppler cooling. The field dependence was particularly puzzling because there seemed to be no reason for the field to have such a large effect. A field of 100 μT (1 gauss) would double the temperature, yet the Zeeman shift caused by such a field (about a megahertz) is much less than the detuning (typically (20 ÷ 30) megahertz). Further experiments [24] also showed that the temperature was linearly dependent on the laser intensity, a dependence that was missed in the earlier NIST measurements [23].

The explanation of these phenomena soon came from groups in Paris [25] and in Stanford [26]. The lectures of Cohen-Tannoudji and others at this Summer School are devoted in large part to this and related phenomena, and the explanation will not be given here. Suffice it to say that the new proposed cooling

mechanisms depend on multiple, normally degenerate ground states that are subject to different light shifts by the molasses laser beams and among which optical pumping establishes population differences. This cooling does not depend upon the Doppler-shift-induced differences in photon scattering rates that are responsible for Doppler cooling. In the particular cases first considered in detail [25, 26] the cooling also depends on a gradient of polarization of the light field, *i.e.* a spatially varying polarization, with the variation being on a wavelength scale. For this reason, the new cooling mechanism has often been called «polarization gradient cooling». In fact, the mechanism is more general than that, as outlined by DALIBARD *et al.* in an even earlier publication on the subject [27]. It encompasses cooling without polarization gradients but in the presence of a magnetic field [28, 29]. This subject is discussed in the lectures of METCALF and NIENHUIS at this Summer School. Here we will deal only with experiments involving polarization gradients.

The new mechanisms explained many of the features of optical molasses that were inconsistent with the old theory of Doppler cooling. One of the major predictions of the new theory (valid for low saturation and large detuning) is that the temperature is proportional to the light shift induced by the molasses laser beams [25]. That is

$$k_B T \sim \frac{\Omega^2}{|\delta|}, \tag{24}$$

where the square of Rabi frequency is proportional to the laser intensity.

This expression explains the sub-Doppler temperatures, because at large enough detuning or low enough intensity the temperature can go below the Doppler-cooling limit. It also agrees with the observed linear dependence of the temperature on laser intensity and, at least qualitatively, the decrease of temperature with increasing detuning. The observed dependence of temperature on polarization is explained by the necessity of having a polarization gradient. Polarization configurations having less polarization gradient produce less cooling. The insensitivity to imbalanced intensity of opposing beams is explained qualitatively by the fact that the friction coefficient is predicted to be significantly larger than for Doppler cooling. The odd dependence on magnetic field is also qualitatively explained. The Zeeman shifts and Larmor precession caused by the field compete with the light shifts and optical pumping needed for cooling. When the magnetic frequencies are significant compared to light shifts and optical-pumping rates, they interfere with the cooling process. Since the light shifts and pumping rates can be rather small at large detuning, the magnetic field needed to interfere with the cooling can be quite small.

7·3. *Experiments with polarization gradient cooling.* – Besides explaining a number of previously unexplained phenomena associated with laser cooling below the Doppler limit, the theory of polarization gradient cooling makes specific

predictions that can be examined experimentally. Unfortunately, most of the experiments have been done in 3-D optical molasses of alkali atoms, while the theory was developed for 1-D cooling of atoms having simpler transition schemes. One particular limitation of these experiments is that it is impossible to have continuous laser beams in a 3-D configuration without a polarization gradient. 1-D collimation of a metastable helium beam [27] showed a distinct difference between cooling with and without a polarization gradient, but, because the transition is narrow and the recoil energy of such a light atom is so large, the difference is not dramatic. Experiments at Stanford [28] used a 3-D sodium molasses, then switched to a 1-D molasses, followed by a time-of-flight measurement of the velocity along the 1-D axis. These experiments clearly showed a temperature somewhat higher than the predicted Doppler temperature when the 1-D molasses had no polarization gradient, and temperatures at least a factor of 10 lower with a polarization gradient (see fig. 5 and 13 of [28]). The dependence of temperature on laser detuning in these experiments was qualitatively in agreement with the predictions of Doppler cooling and of polarization gradient cooling for the cases without and with polarization gradients, respectively. Other 1-D experiments with various configurations of polarization have been performed by laser collimation of a rubidium beam at Stony Brook [29].

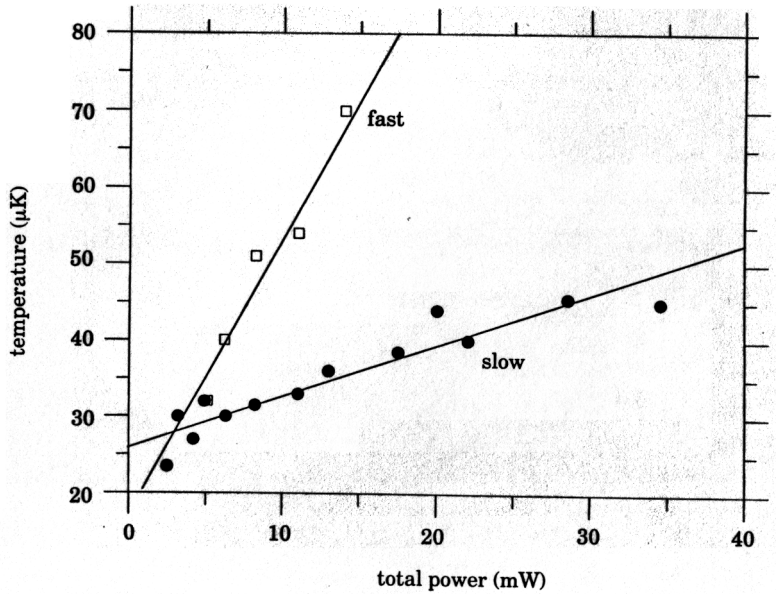

Fig. 10. – Temperature as a function of laser intensity for fast and slow turn-off of the laser beams.

The clear difference between cooling with and without a polarization gradient is convincing evidence in support of the new theory. Another convincing, though qualitative, test involved the influence of a magnetic field on the temperature. Recall that the explanation of the increased temperature with increased field involved the magnetic field competing with light shifts and optical-pumping rates. If correct, this would imply that an optical molasses with higher-intensity laser beams should be less sensitive to a magnetic field than one with weaker beams. Exactly this dependence was confirmed (see ref. [19], fig. 19).

The linear dependence of the temperature on the laser intensity leads to an interesting phenomenon [19], illustrated in fig. 10. This shows the temperature for a sodium molasses, measured by time of flight, as a function of the total laser power under two different conditions for the release of the molasses. In the one instance (open squares) the laser intensity was turned off rapidly (about 100 ns) and in the other (filled circles) it was turned off slowly (about 20 μs). In both cases the temperature depends linearly on the intensity, but the slow turn-off gives a lower temperature. The reason is that during the slow turn-off the atoms come to equilibrium at the lower temperatures appropriate to the lower intensity. For the fast turn-off there is insufficient time for such equilibration. This suggests still another experiment [19] in which the turn-off time t_r is varied so as to determine the equilibration time for the polarization gradient cooling. The results of such an experiment are shown in fig. 11. For very short turn-off times, between 0.1 and 1 μs, the temperature hardly varies, but, between 1 and 10 μs, the temperature drops dramatically, suggesting that the characteristic time for equilibrating the temperature is around 3 μs. This is to be compared to a minimum time of 40 μs predicted by the Doppler-cooling theory, eq. (19). The experiment shows that the friction coefficient α is, as predicted, much larger in polarization gradient cooling than for Doppler cooling.

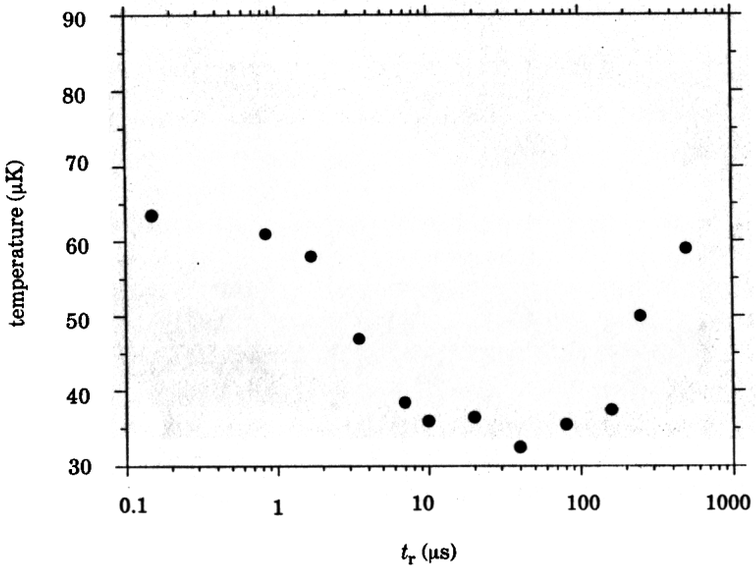

Fig. 11. – Temperature as a function of the time to ramp the laser intensity linearly to zero.

Another important prediction of the theory is that there is a threshold intensity for which the polarization gradient mechanism will work. At first glance this may seem to be a trivial statement, since surely the process will not work with zero laser intensity. Nevertheless, the existence of a threshold is very different from the situation with Doppler cooling. Equation (18), for example, shows that the temperature in Doppler cooling goes to a constant as the intensity approaches zero. For polarization gradient cooling, however, the temperature decreases according to eq. (24) until the threshold intensity is reached. At this point, the polarization gradient mechanism becomes ineffective and the spread of the velocity distribution is predicted to increase sharply [30]. Roughly speaking, the temperature of the atoms is about equal to the light shift induced by the laser beams until that light shift becomes comparable to the recoil energy of the atoms. At that point the cooling mechanism ceases to be effective (the phenomenon of *décrochage*, literally, «becoming unhooked»). This threshold behavior is described in detail in ref. [1] and in ref. [30].

Some initial indication of this threshold effect or *décrochage* is already seen in the data of fig. 11. The temperature is seen to rise when the turn-off time becomes very long. The interpretation is that for long turn-off times the atoms spend a significant length of time with the laser intensity below the threshold. During this time the atoms heat up, so the observed temperature rises. This was seen more explicitly in an experiment [19] where a 3-D optical molasses was loaded at high intensity and then the laser intensity was suddenly switched to a lower value. After a period of equilibration the temperature was measured by TOF. As expected, the observed temperature went down as the intensity was made lower. But, once the intensity was lowered below a critical value, the temperature started to increase again. Furthermore, when a low-temperature sample of atoms (initially cooled by sufficiently intense laser beams) was exposed to an optical molasses with intensity well below the critical intensity, the atoms' temperature was observed to increase, presumably toward the Doppler temperature. More direct observation of the threshold effect was made in experiments in Paris, described below.

Another prediction of the theory was the inverse dependence of temperature on detuning. Results on sodium as in fig. 9 show the inverse dependence qualitatively, but for large detuning where the theory should be most accurate the temperature is flat or possibly increasing with increased detuning. This is

ot very surprising in the case of sodium because the cooling transition, $S_{1/2}(F=2) \rightarrow 3P_{3/2}(F=3)$, is only 60 MHz higher in frequency than the $S_{1/2}(F=2) \rightarrow 3P_{3/2}(F=2)$ transition. Thus, when the detuning exceeds 0 MHz as in fig. 9, the laser is actually tuned closer to the other, unwanted ransition than to the desired cooling transition. The presence of the other tran- ition presumably leads to some extra heating. Experiments with cesium avoid his problem because the corresponding unwanted transition is 250 MHz away rom the cooling transition and the natural linewidth is about 5 MHz, a factor of wo smaller than in sodium. Thus, relative to the linewidth, the unwanted tran- ition is more than eight times farther away in cesium than in sodium.

At ENS in Paris experiments with a 3-D molasses of cesium [27] had seen ub-Doppler temperatures soon after their discovery in sodium at NIST. Fur- her experiments on cesium provided additional detailed comparisons with the ew theories. Using a technique where the molasses was efficiently loaded at igh intensity and small detuning, then switched to smaller intensity and/or arger detuning, the Paris group measured the molasses temperature for a wide range of intensity and detuning [31]. The results are shown in fig. 12. Here we ee the linearity of temperature with laser intensity, as had been observed in odium, and also the inverse dependence on detuning. In fact, nearly all the

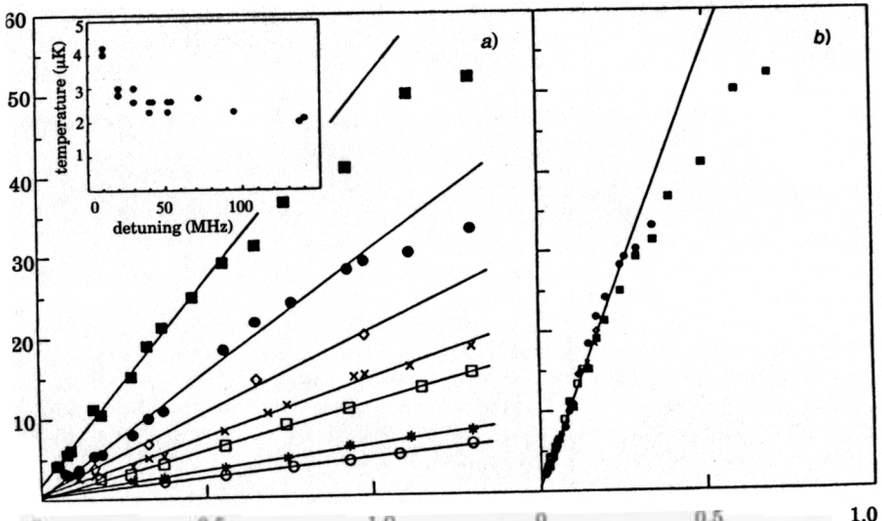

Fig. 12. – *a*) Temperature as a function of the (single beam) intensity for various detunings. *b*) Temperature as a function of I/δ. Inset: Lowest observed temperature as a function of detuning.

data are well represented by eq. (24), and the temperature is seen to depend on the single parameter I/δ. Only at large intensity and small detuning (where eq. (24) is not valid) does the temperature deviate from linearity in this parameter.

Of particular interest in fig. 12 is the lowest temperature reached. For each detuning there was an intensity below which the molasses did not function, as expected from the theory. Once the detuning was more than a few linewidths from resonance, this point of *décrochage* (where the cooling fails to work) occurred at a constant value of I/δ, *i.e.* at constant light shift and, therefore, at constant temperature. The lowest temperature seen was always about 2.5 μK, corresponding to a r.m.s. velocity along a given axis of 1.3 cm/s, a bit more than three times the recoil velocity. Similarly, the lowest temperature seen for a sodium molasses is about 25 μK [19], also corresponding to just over three recoil velocities. All of this is at least qualitatively consistent with the expectations concerning the threshold intensity and the polarization gradient cooling limit (see the lecture of COHEN-TANNOUDJI for this Summer School and ref. [30]). Furthermore, the actual values of the temperatures observed in fig. 12 are about a factor of three larger than the temperatures predicted in 1-D for a simpler, $J = 1/2 \rightarrow J = 3/2$ transition in the linear domain where eq. (24) is valid. The factor of three can easily be rationalized from the fact that the average light intensity in the 3-D configuration, with three times as many laser beams, is three times as large. Considering the difference in the transition schemes, and the fact that no complete theory of the 3-D situation has been worked out, the agreement is quite remarkable.

7·4. *Outlook for optical molasses.* – The new cooling mechanisms, of which polarization gradient cooling is the paradigm, have brought about a revolution in laser cooling of neutral atoms. As it now appears, the ultimate temperature achieved in optical molasses has very little to do with the original Doppler-cooling idea as presented in sect. 2-5 (although Doppler cooling probably plays a role in getting the atoms into the molasses). Furthermore, the laser cooling works much better than ever hoped for Doppler cooling. The unexpected low temperatures have opened practical applications for laser cooling that were elusive or speculative before the appearance of the sub-Doppler temperatures. Among these is the use of laser-cooled atoms in an atomic-fountain clock.

The idea of a fountain clock, first proposed by ZACHARIAS in 1953 [32], is that atoms are launched vertically through a resonant cavity where they are put into a superposition state between the two states comprising the clock transition. After passing through the cavity the atoms fall back, traversing the cavity once more, with the cavity field acting on the superposition state to produce the Ramsey separated oscillatory-field interference (described in more detail in the lecture by RAMSEY at this Summer School). The advantage of such a fountain over conventional (usually horizontal) atomic-beam clocks using the Ramsey

technique is that the interaction time is longer so the linewidth is narrower. Furthermore, the double passage through the same cavity (in contrast to the conventional case where two cavities are traversed in succession) can result in the cancellation of certain systematic errors [33]. Interest in such fountain clocks was revived by the advent of laser-cooling techniques, but, before polarization gradient cooling and its extremely low temperatures, the atomic fountain was not really practical. Now, Cs r.m.s. velocities near 1 cm/s mean that fountains with round trip times on the order of 1 s are possible without unacceptable spreading of the atomic sample.

The first atomic fountain was demonstrated at Stanford [34] with sodium, although not in exactly the manner described above. A Cs fountain experiment in the manner suggested by ZACHARIAS was recently achieved in Paris [35]. It now seems likely that a clock using such a fountain will be the ultimate cesium time standard.

In spite of all these successes, there is much about optical molasses that is not well understood. Super molasses [21] has never been satisfactorily explained. Whether it represents a trap or an exceptionally strong viscous confinement is not clear. The molasses lifetime, the time atoms are held in a molasses, is not understood in the context of the new cooling mechanisms, nor is it even clear that the motion of atoms in optical molasses is even diffusive. Purely Doppler molasses has not been observed in three dimensions, and it remains to be seen whether it will work very well, or at all. Much remains to be done in laser cooling of neutral atoms, theoretically, experimentally and in practical applications.

8. – Traps for neutral atoms.

Confinement of atoms by electromagnetic forces has long been an appealing experimental goal. The successes of ion traps (see, for example, the lectures of PAUL, WINELAND and WALTHER for this Summer School) are a testament to the power of the technique. Trapping neutral atoms is harder, because, without a charge to act upon, the trapping forces must rely on interactions with higher-order moments, typically dipole moments. This results in comparatively weak forces and shallow traps. Various kinds of traps have been proposed or realized over the years, using magnetic, electric and optical fields in both static and dynamic configurations, and in various combinations. Some of this is reviewed in ref. [3].

The concept of magnetostatic trapping of neutrals was first proposed by PAUL (see his lecture at this Summer School). PAUL was the first to demonstrate the trapping of a neutral particle, the neutron, using a geometry suggested by HEER [36]. The first electromagnetic trap for neutral atoms was a magnetostatic spherical quadrupole trap for Na demonstrated at NIST [37]. Later magnetostatic traps used linear multipole fields with pinched ends to trap

Na [38] and H [39]. More recently, the first magnetodynamic trap was demonstrated at JILA (see the lecture by WIEMAN at this Summer School, ref. [40] and the references therein). Below we will treat only optical traps and the position-dependent forces needed to produce a trap.

9. – Radiation pressure traps.

9·1. *Separated-focus traps.* – Trapping requires a position-dependent force. One way of achieving this with the radiation pressure force described by eq. (1) is to have the intensity of the light vary with position. ASHKIN proposed a simple geometry [41], shown in fig. 13, for a 1-D trap. The figure represents two counterpropagating laser beams with circular cross-section.

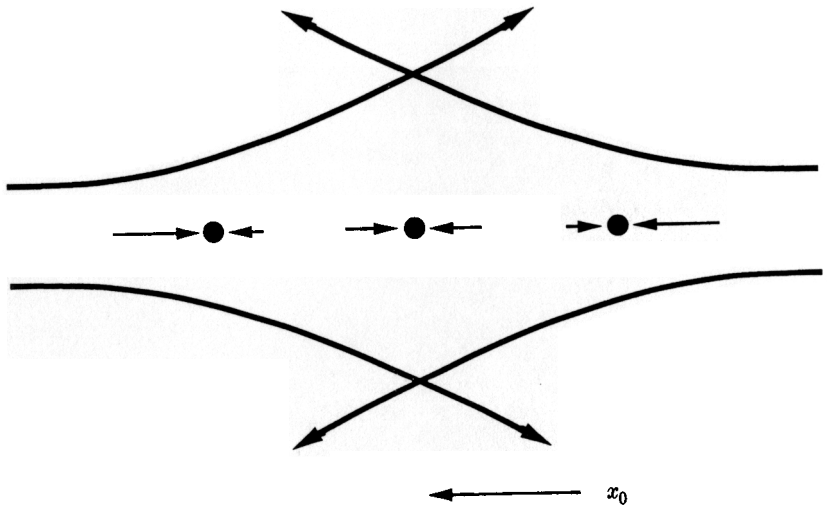

Fig. 13. – Ashkin's radiation pressure force trap formed from two opposed focussed laser beams with separated foci.

At the trap center, equidistant from the two foci, the forces from the two beams balance, while an atom that moves off center along the x-axis (the symmetry axis or axis of laser propagation) feels a restoring force from the higher-intensity beam. For moderate intensity ($I/I_0 \lesssim 1$) we may approximate the force on an atom by the sum of the forces from each beam, given individually by eq. (1). If the distance x_0 from the trap center to the foci is greater than or of the order of the confocal distance (the distance from the focus where the Gaussian beam radius is $\sqrt{2}$ greater than the radius at the focus), we find the derivative

of the force at the trap center to be

$$\frac{dF_x}{dx} \equiv \kappa \approx \frac{I}{I_0}\frac{\hbar k \Gamma}{x_0}, \tag{25}$$

where κ is the spring constant and I is the intensity at the trap center. The oscillation frequency in this 1-D trap is

$$\omega_{trap} = \sqrt{\frac{\kappa}{M}} \approx \sqrt{\frac{I\hbar k\Gamma}{I_0 M x_0}} = \sqrt{\frac{I v_{rec}\Gamma}{I_0 x_0}}. \tag{26}$$

For sodium, with $x_0 \approx 1$ cm and $I/I_0 \approx 1$ this radian frequency is $\sim 10^4\,s^{-1}$; it is about 4 times smaller for cesium.

The «static» (force calculated for zero atomic velocity) longitudinal depth of the trap is just the integral of the force out to some distance, which we can take to be of the order of x_0. Assuming the force to be approximately linear over this distance, we find for $I/I_0 \approx 1$

$$U_{trap} \approx \hbar\Gamma\frac{x_0}{\lambda} \approx k_B T_{Dop}\frac{x_0}{\lambda}, \tag{27}$$

where λ is the optical wavelength and we have generally suppressed numerical factors. Since $x_0 \gg \lambda$ in general, the trap is deep compared to the Doppler-cooling limit, and, therefore, should be stable if tuned so as to provide Doppler cooling. The «dynamic» trap depth would include the possibility of a velocity-dependent damping force, and could be greater than the static depth.

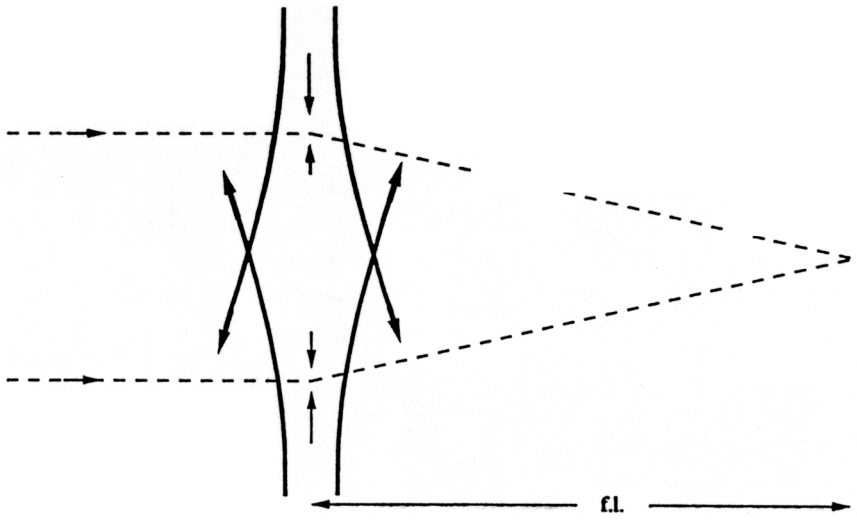

Fig. 14. – Radiation pressure 1-D lens.

The configuration shown in fig. 13 has been used as a 1-D lens for a neutral atomic beam, as shown in fig. 14 [42,43]. Such lenses are discussed in the lecture by BALYKIN at this Summer School, and also in the lecture of PRITCHARD and KETTERLE.

9·2. *Optical Earnshaw theorem.* – While the 1-D trap can act as a lens, it is not really a trap since it cannot confine atoms in all directions. In fact, it is easy to see that the 1-D trap actually expels atoms that are displaced slightly in the direction perpendicular to the laser propagation (x) axis. We can extend the configuration to 2-D, as shown in fig. 15.

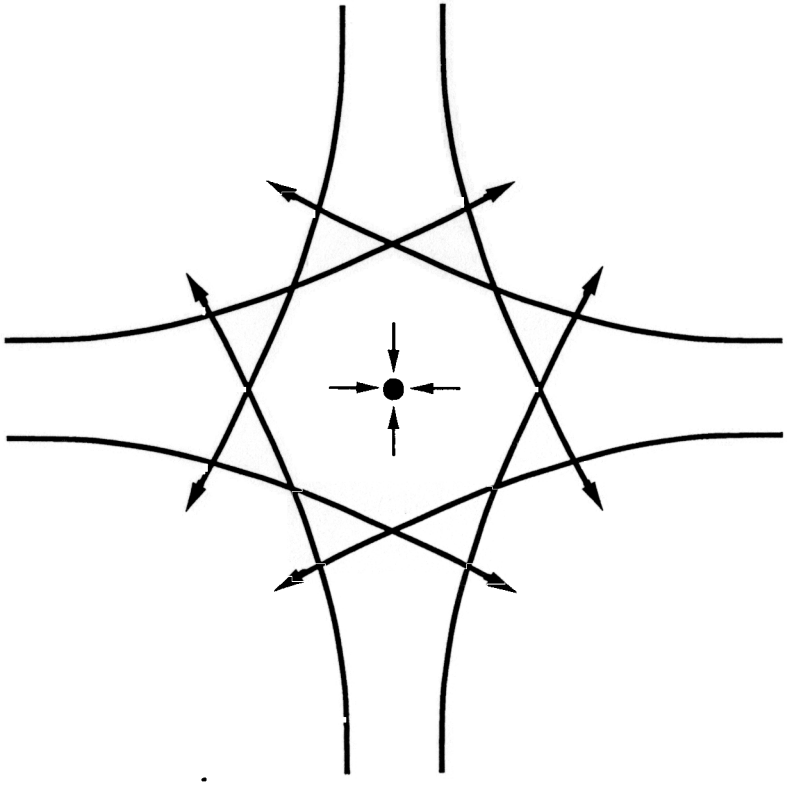

Fig. 15. – Radiation pressure trap in 2-D, formed by four focussed beams of circular cross-section.

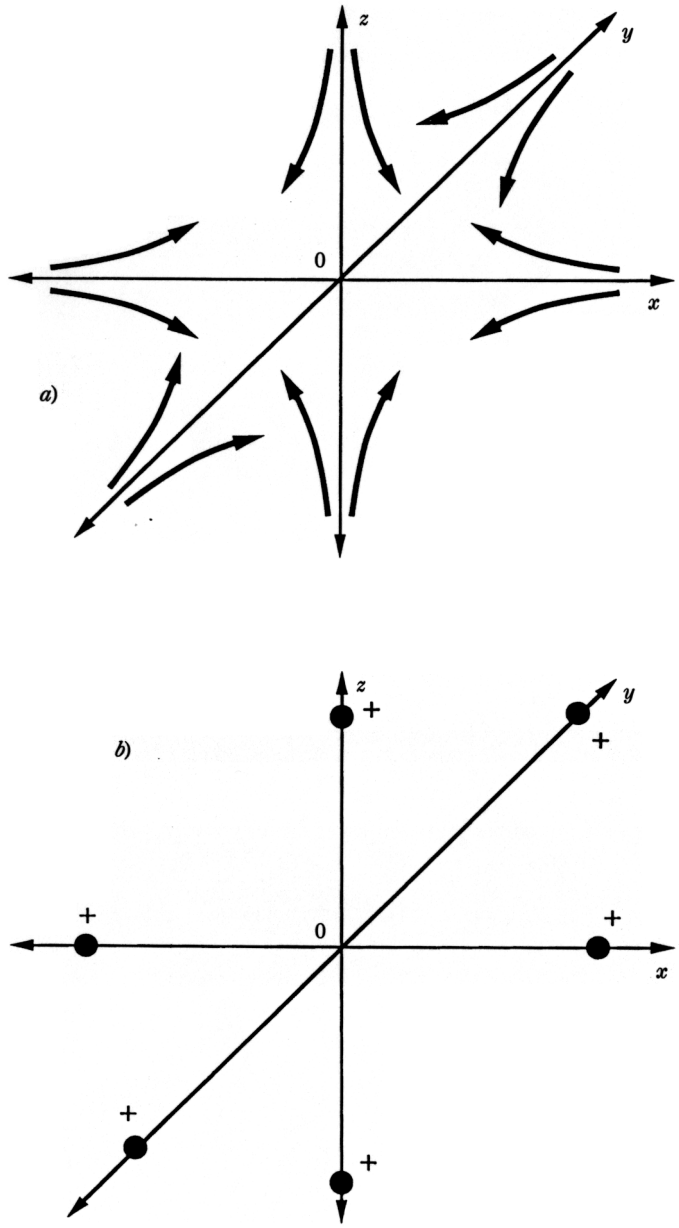

Fig. 16. – *a*) 3-D optical «trap». *b*) Electrostatic analog.

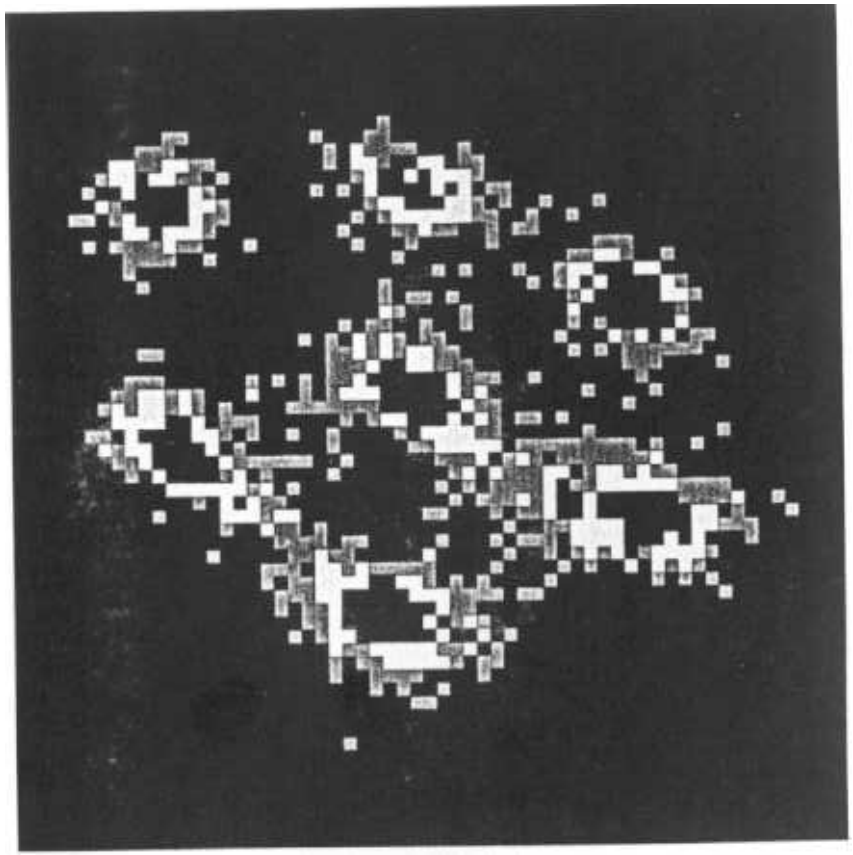

Plate I. – Ordered ion structure in a Paul trap formed under the influence of laser cooling. The average separation of the ions is 20 μm (photo courtesy of H. WALTHER, Max-Planck-Institut für Quantenoptik, Garching).

For any small displacements from the trap center in the plane of the page, there is a linear restoring force. However, displacements perpendicular to the page result in an expelling force in that direction. It is reasonable to consider whether this expelling force can be eliminated by extending the configuration to 3-D. That configuration is shown in fig. 16*a*). In spite of the obvious appeal of such a configuration, it is not in fact a trap. This was shown explicitly by ASHKIN and GORDON [44], who also proved a general theorem, called the optical Earnshaw theorem by analogy with the theorem forbidding a stable equilibrium for a charged particle in electrostatics. The basic idea of the optical Earnshaw theorem can be understood by considering that for low intensity the force on an atom near the origin in fig. 16*a*) is analogous to the force on a positive test charge at the origin of fig. 16*b*), where positive charges on the coordinate axes play the role of laser beams with foci on the axes. Because the divergence of $\boldsymbol{E}$ is zero, the electrostatic case cannot be a stable trap. Analogously, the divergence of the Poynting vector is zero (the light flux cannot point inward everywhere), so the light trap cannot be stable.

The optical Earnshaw theorem is in fact more general than this, and applies as long as the force on an atom is linear in the applied optical intensity, and the optical field is static. The optical Earnshaw theorem is discussed in the lecture of PRITCHARD and KETTERLE at this Summer School.

The theorem only applies to the radiation pressure force, and not to the «dipole» or «gradient» force (see sect. **10**). A number of ways of circumventing the Earnshaw theorem for radiation pressure forces have been proposed. One method [45, 46] is to use time-varying optical fields in analogy to the r.f. or Paul trap for ions, although there may be a problem because Doppler cooling damps the micromotion which is needed to produce stability in such a trap [46]. Another approach is to use a configuration where the force is not linear in the intensity because of spatially varying optical fields, or because of special optical-pumping arrangements [47]. But the clear winner among post-Earnshaw theorem radiation pressure traps is the magneto-optic trap.

9·3. *Magneto-optic trap* (MOT). – The magneto-optic trap (MOT), also called Zeeman assisted radiation pressure trap (ZARPT), Zeeman assisted optical trap (ZOT), opto-magnetic trap or magnetic molasses, was first proposed by DALIBARD [48] in a 1-D configuration. It was first demonstrated as a 3-D trap by RAAB *et al.* [49]. The principle in its simplest form is illustrated in fig. 17. Two counterpropagating laser beams with opposite directions of circular polarization act on a $J = 0 \rightarrow J = 1$ transition in the presence of a magnetic field directed along the laser axis, whose magnitude is proportional to the distance from the trap center and whose direction reverses at the trap center. The magnetic sublevels and the helicities of the laser beams are labelled according to a space-fixed axis, in this case the positive z-axis.

The basic idea, within the context of Doppler cooling, is that for a red de-

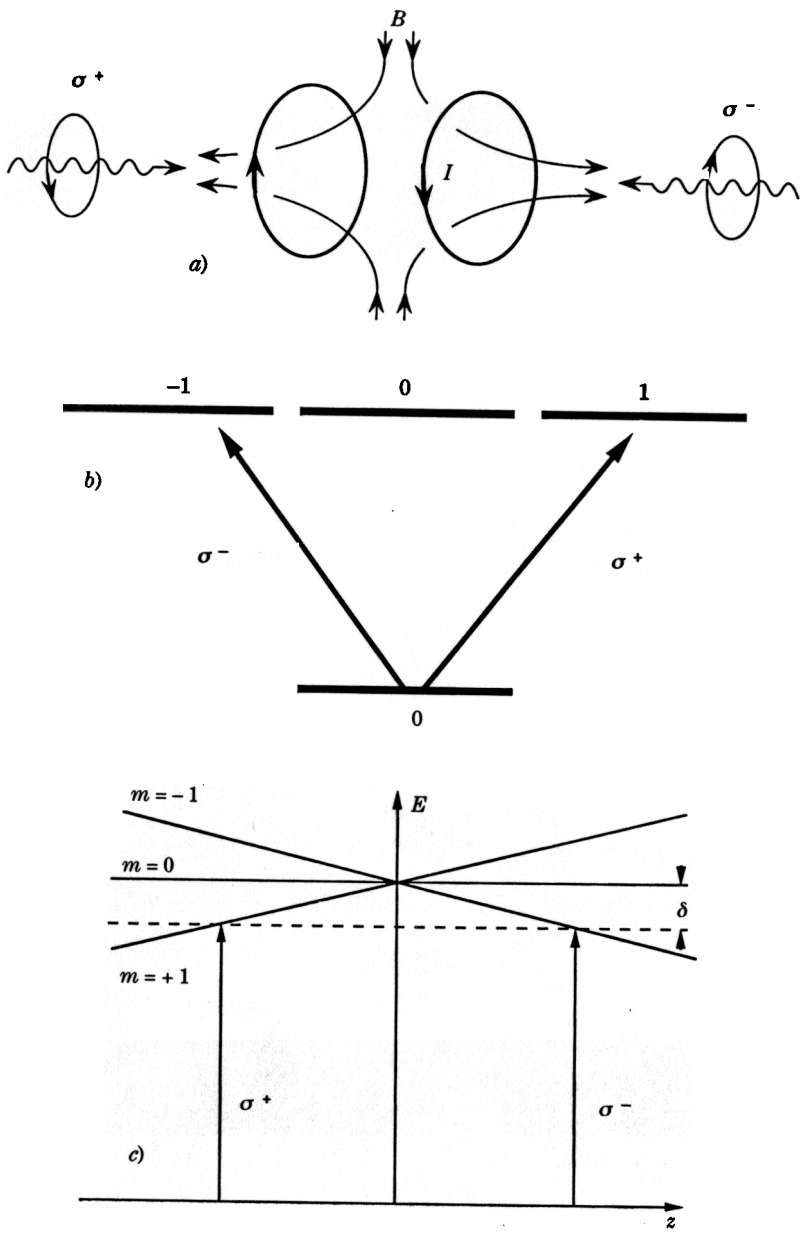

Fig. 17. – *a*) 1-D MOT. *b*) Transition scheme. *c*) Energy levels in the spatially varying field.

tuned laser frequency, an atom displaced from the origin is acted upon by the laser beam which tends to push it back to the origin. The beam of opposite polarization, which would push the atom away from the origin, is out of resonance because of the Zeeman shift. We will analyze the trap for the conditions $I/I_0 \ll 1$, $kv \ll 1$, $\mu B/\hbar \ll \Gamma$, where $\mu B/\hbar$ is the Zeeman frequency shift of the upper state. Because the field varies linearly with distance, this frequency shift can be written as $\omega_Z = \beta z$. The total force on an atom in the low-intensity limit is taken to be the sum of the forces exerted by the individual beams:

$$(28)\quad F = F_{\sigma^+} + F_{\sigma^-} = \frac{\hbar k \Gamma}{2}\left[\frac{I/I_0}{1+4\left(\frac{\delta - kv - \beta z}{\Gamma}\right)^2} - \frac{I/I_0}{1+4\left(\frac{\delta + kv + \beta z}{\Gamma}\right)^2}\right]$$

Now we take the small-velocity, small-Zeeman-shift limit:

$$(29)\quad F(v,z) = \frac{2\hbar k(2I/I_0)(2\delta/\Gamma)[kv + \beta z]}{[1 + (2\delta/\Gamma)^2]^2}.$$

This is identical to the expression for the force in optical molasses (eq. (11)), except that kv has been replaced with $kv + \beta z$. The motion of an atom under the influence of this force is that of damped harmonic oscillator:

$$(30a)\quad \ddot{z} + \gamma \dot{z} + \omega_{\text{trap}}^2 z = 0,$$

with

$$(30b)\quad \gamma = \frac{4\hbar k^2 (I/I_0)(2\delta/\Gamma)}{M[1 + (2\delta/\Gamma)^2]^2}$$

and

$$(30c)\quad \omega_{\text{trap}}^2 = \frac{4\hbar k (I/I_0)\beta(2\delta/\Gamma)}{M[1 + (2\delta/\Gamma)^2]^2}.$$

The character of the motion of an atom in the trap is determined by the ratio

$$(31)\quad \frac{\gamma^2}{4\omega_{\text{trap}}^2} = \frac{\hbar k^3 (I/I_0)(2\delta/\Gamma)}{\beta M[1 + 2I/I_0 + (2\delta/\Gamma)^2]^2},$$

where we have added a saturation term to the denominator in the spirit of the treatment of optical molasses in sect. 4, eqs. (13), (14). If this ratio is greater than unity, the motion is overdamped. If we take $2\delta/\Gamma = 1$ and $I/I_0 = 1$ for maximum damping and trap stiffness, we can write

$$(32)\quad \frac{\gamma^2}{4\omega_{\text{trap}}^2} = \frac{\pi E_{\text{rec}}}{4\lambda\hbar\beta}.$$

That is, this ratio is essentially the ratio of the recoil energy to the change in Zeeman energy over an optical wavelength. A typical experimental value for β corresponds to 10 G/cm (14 MHz/cm). This leads to a $\gamma^2/4\omega_{\text{trap}}^2$ of about 25 for sodium and 1.4 for cesium. Thus it appears that the MOT will be overdamped, particularly for light atoms, unless, for example, the detuning is large or the intensity is small.

With the above choice of parameters the oscillation frequency is given by $\omega_{\text{trap}}^2 = \beta v_{\text{rec}}/4$. This is a radian frequency of $8 \cdot 10^3\,\text{s}^{-1}$ or about a kilohertz for sodium. The well depth at 0.5 cm is about 2 K for these parameters in Na. These are about the same frequency and depth we would get for the 2-focus laser trap of fig. 13 because both that and the MOT rely on radiation pressure. We note that in both cases we have spoken only of the static depth of the trap, the energy required to slowly displace an atom a given distance from the equilibrium point. An atom with a given kinetic energy at the trap center will also experience Doppler cooling, so that the kinetic energy of an atom that can remain trapped is even greater than the static depth of the trap.

Here we have treated the MOT only in 1-D and with a nondegenerate ground state (this eliminates the possibility of polarization gradient cooling, which requires a degenerate ground state). Experimentally the MOT functions very well in 3-D and with multilevel atoms. The 3-D configuration is as in fig. 17*a*), with additional circularly polarized laser beams along the orthogonal coordinate axes. Color plate III shows such a MOT for Na. There is no general theory of a 3-D MOT in a realistic configuration. Observations indicate that the 3-D MOT may function even when some of the polarizations are not as prescribed for the 1-D MOT. This is not understood at present. STEANE and FOOT [50] have found that the temperature of atoms in a MOT can be below the Doppler-cooling limit, indicating that polarization gradient cooling forces are operating. STEANE and FOOT considered an analysis of the problem in analogy to the $\sigma^+ - \sigma^-$ cooling on a $J = 1 \rightarrow J = 2$ system treated by DALIBARD and COHEN-TANNOUDJI [25]. In the expression derived in [25] the term kv is replaced with $kv + \beta z$, just as in the treatment above. In the context of polarization gradient cooling this results in an increase of both the cooling force and the trapping force, in the same proportion. The experiments of ref. [50] showed that both the trapping and the cooling were greater than expected for a MOT with a nondegenerate ground state, but a detailed comparison with theory was not possible because of the more complicated, 3-D character of the experiment. This and other experiments are discussed in the lecture of FOOT for this Summer School.

The 3-D MOT, along with optical molasses, has become an important tool in neutral-atom laser cooling. It is particularly useful in collecting atoms from an atomic beam cooled by the Zeeman tuning technique and has been used to trap even rare isotopes of metastable atoms [51]. The trap can collect the slow atoms from an uncooled thermal distribution [52], and is able to concentrate the atoms so much that collisions [53] and radiation pressure exerted by the atoms' fluorescence [54] are factors limiting the achieved density. In 2-D the MOT has been used as an «atomic funnel» to concentrate sodium atoms both with near zero longitudinal velocity [55] and in an atomic beam with 50 m/s longitudinal velocity [56].

10. – Dipole force and dipole force traps.

The dipole force (also called the gradient force or stimulated force) was first proposed as a means of trapping atoms by LETOKHOV in 1968 [57]. This force can be thought of in a number of different ways, some of which we will briefly recount.

The dipole force can be considered as arising from absorption followed by stimulated emission, as distinguished from the radiation pressure force which may be thought of as absorption followed by spontaneous emission. (Note that the absorption and stimulated emission in the dipole force cannot be thought of as successive and independent events; their correlation is central to the proper understanding of the force.)

We can also understand the dipole force in analogy to a driven classical oscillator. A harmonically bound charge driven by an oscillating electric field has an oscillating dipole moment which is in phase with the driving field when driven below resonance and out of phase when driven above resonance. The energy of interaction between dipole and field is $W = -\boldsymbol{\mu} \cdot \boldsymbol{E}$. Below resonance the energy is negative and the oscillator will be drawn toward a more intense field, while above resonance it will be drawn to the weaker part of the driving field.

Another physical understanding of the dipole force (due to ASHKIN) is illustrated in fig. 18. Consider a laser beam with a Gaussian intensity profile incident on a refractive sphere with index greater than one. Ignoring reflection, we see that, when the center of the sphere is in a gradient of the light intensity, more light is refracted toward the direction of lower intensity, so the sphere recoils toward high intensity. For $n < 1$ the reverse is true. Since the index of refraction of a gas in the vicinity of a resonance is as shown in fig. 18*c*), we may conclude that atoms irradiated below resonance will be drawn to the stronger part of the optical field, just as we concluded for the driven oscillator. This image emphasizes the nondissipative nature of the dipole force.

10·1. *Dressed-atom picture.* – A particularly appealing way of understanding the dipole force is in the dressed-atom picture. A detailed treatment of this is given by DALIBARD and COHEN-TANNOUDJI [58]. We present the basic ideas here. Consider a 2-level atom with states $|g\rangle$ and $|e\rangle$. Separately consider a single mode of the radiation field, close to resonance with the atomic transition, having energy levels labeled $\ldots |n-1\rangle, |n\rangle, |n+1\rangle, \ldots$ according to the number of photons in the mode. The energy levels of these two distinct systems are shown in fig. 19*a*) for the case where the photon energy ω_L is greater than the

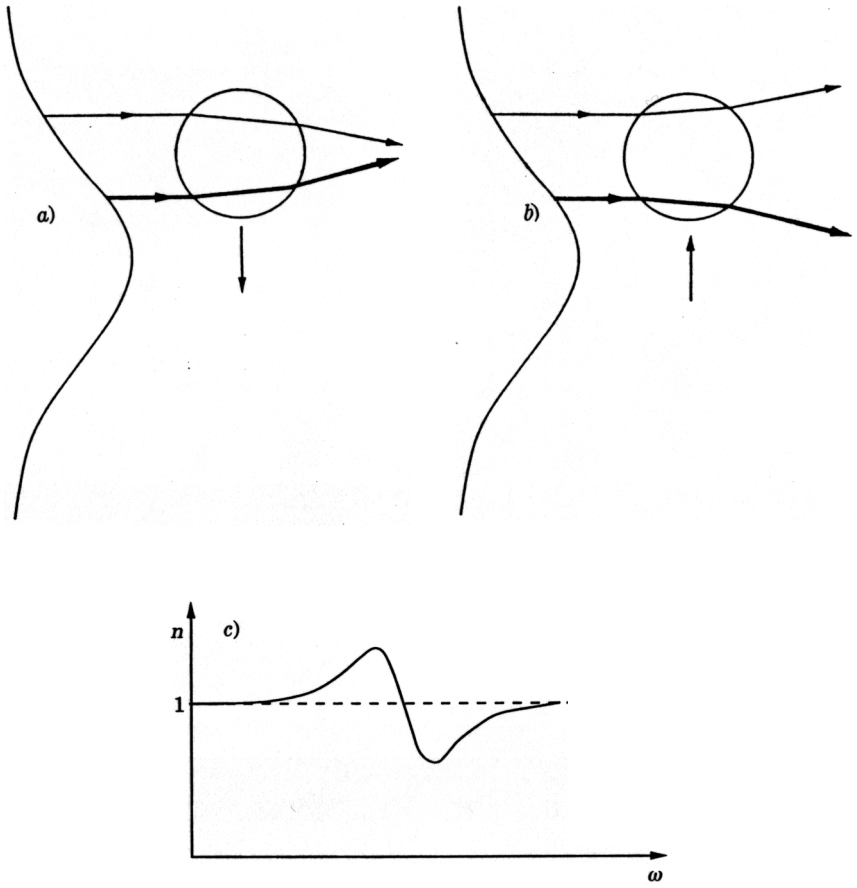

Fig. 18. – Refraction of a Gaussian laser beam by a sphere of index greater than 1 (*a*)) and less than 1 (*b*)). *c*) shows the index of a gas in the vicinity of a resonance.

difference in energy between the atomic states, ω_A. This is the «bare» basis in which we consider the atom's energy levels and those of the photon field separately. Now let us consider the «dressed» basis (atom dressed by photons) where we take the total energy of the atom plus the field. This is shown on the left-hand side of fig. 19*b*). We have a ladder of dressed states, with each double rung corresponding to a ground-state atom together with a certain number of photons and a nearly degenerate state with an excited atom together with one

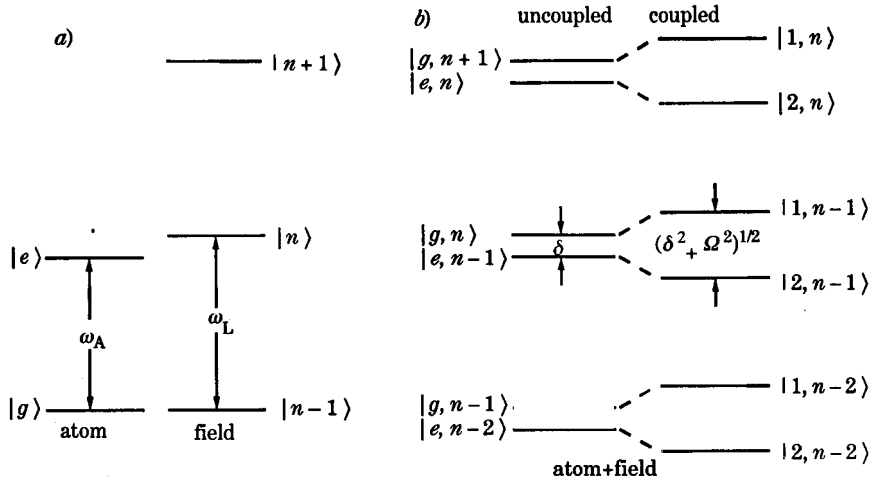

Fig. 19. – *a*) Energy levels of the atom and the field in the bare basis. *b*) Dressed basis of atom + field, with the atom uncoupled and coupled to the field.

less photon. The separation between the nearly degenerate levels is the detuning δ and the separation between corresponding rungs on the ladder is ω_L.

At this point we have simply added the energies of the atom and of the field, without considering any energy of interaction between the atom and the field. Turning on this interaction, with a strength characterized by the Rabi frequency Ω, we get the right-hand side of fig. 19*b*). The closely spaced energy levels are repelled by the interaction, and are now separated by $(\delta^2 + \Omega^2)^{1/2}$, which is often called the generalized or effective Rabi frequency. (See the lecture of RAMSEY for this Summer School for a discussion of these frequencies in the context of magnetic resonance.) The interaction mixes the closely spaced levels together, so that each of the new levels has both ground- and excited-state character. Therefore, the labeling in the coupled basis has been changed to $|1, n\rangle$ and $|2, n\rangle$, with n indicating the number of photons associated with the excited state in the uncoupled basis.

The atom can make transitions between the rungs on the ladder of dressed levels by the spontaneous emission of photons. Because each level has both excited- and ground-state character, the spontaneous transitions can change the nature of the level of the atom. It is through this process that an average distribution of population between the two types of levels is established, a distribution depending on the detuning, the decay rate and the Rabi frequency.

The repelling of levels caused by the interaction of atom and field is the origin of the dipole force in this picture. Consider a light field, such as a focussed laser beam with a Gaussian intensity profile, where the intensity varies in

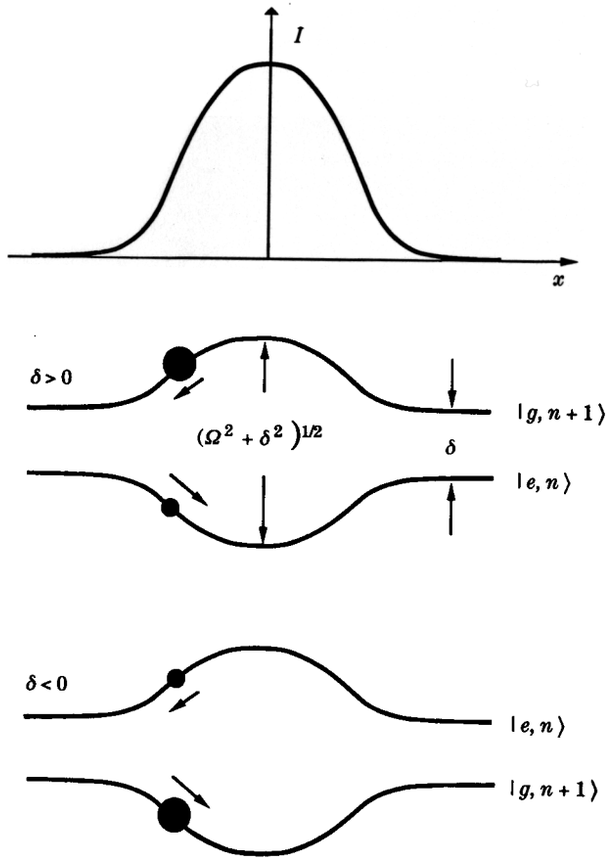

Fig. 20. – Top: The intensity profile of a Gaussian laser beam. Bottom: The dressed-level potentials as a function of position for this intensity profile, for detuning above and below resonance. The sizes of the black dots indicate the relative population of the states.

space. This means that the Rabi frequency and thus the energy of interaction varies in space. Figure 20 illustrates this situation. Where the laser intensity is small, and the dressed levels are approximately described by ground or excited state, the separation of the dressed levels is minimal and equal to the detuning δ. Where the laser intensity is maximum, so is the dressed-state separation.

For any finite laser intensity the dressed state that is connected to the ground state will be more heavily populated. When $\delta > 0$, this is the state of

higher energy, so an atom in that dressed state is repelled from the region of high intensity, as shown in the figure. Of course, the atom spends some of its time in the other dressed state, attracted to the high intensity, but on average it is repelled. It is the population weighted average of the two dressed-state potentials that constitutes the «dipole potential». For $\delta < 0$ the situation is just reversed and the atom is, on average, attracted to the high intensity. For negative detuning, then, a focussed laser beam is a trap, attracting the atom to the focus, the point of maximum intensity.

For zero detuning the average dipole potential is zero, even though each individual dressed-state potential has the maximum variation. This is because the population is evenly distributed between the two dressed states. Let us consider the interesting case where the spontaneous emission is turned off. Then the population of the two dressed levels does not come to equilibrium and an atom on one of the dressed levels can experience the potential of that dressed level rather than the average dipole potential. This case was considered in ref. [59]. The well depth of the two dressed-state potentials is

$$U = \pm \frac{\hbar}{2}[\delta - (\delta^2 + \Omega^2)^{1/2}]. \tag{33}$$

It is maximum at zero detuning, but the potential is only useful as a trap if the atom stays on a single dressed level, *i.e.* in the absence of spontaneous emission.

10·2. *Practical dipole traps.* – The dipole force may be derived from a potential [11-13], which we re-write here as

$$U = \frac{\hbar\delta}{2} \log\left[1 + \frac{I/I_0}{1 + (2\delta/\Gamma)^2}\right]. \tag{34}$$

If we assume we interact with sodium atoms using the strongest transition ($I_0 = 6\ \mathrm{mW/cm^2}$), a 10 mW beam with a Gaussian intensity profile focussed to a $1/e^2$ radius of 10 μm gives $I/I_0 = 10^6$ at the center of the focus. For the detuning maximizing U we find $U_{\max}/k_B \approx 100$ mK. For a 1 W beam we have $I/I_0 = 10^8$ and $U_{\max}/k_B \approx 1$ K. If such a potential is used to make a trap, it can, then, have a depth comparable to that of the radiation pressure traps described above. However, a dipole trap typically requires greater laser power and much greater intensity than a comparably deep radiation pressure trap, so it must be focussed to an extremely small size.

Figure 21 shows the dipole potential as a function of detuning, with both variables effectively normalized to the Rabi frequency. For high intensity the curves are universal, and the potential is maximized [12] when the saturation parameter $s = (I/I_0)/(1 + (2\delta/\Gamma)^2) \approx 4$. A trap can easily be made using this dipole potential. The first and probably simplest example is a laser beam of

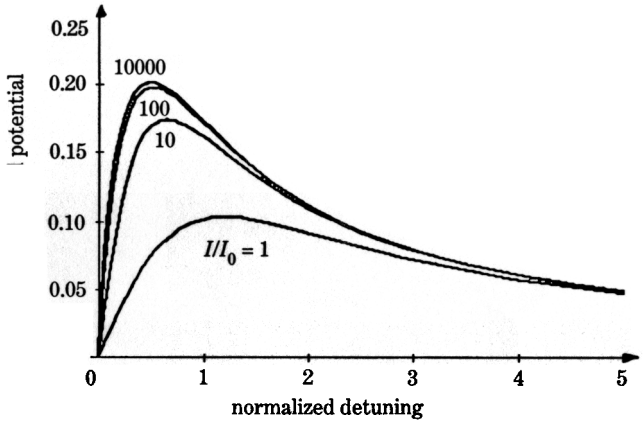

Fig. 21. – Normalized dipole potential $U/\hbar\Gamma'\sqrt{I/I_0}$ as a function of normalized detuning $2\delta/\Gamma'\sqrt{I/I_0}$.

Gaussian cross-section, brought to a single focus. Proposed by ASHKIN [41], it was first demonstrated at Bell Labs [60]. The laser intensity has an absolute maximum at the center of the focus, giving a trap whose depth is just the optical potential at that point (if we ignore the radiation pressure). Can such a trap be stable in the sense that it has a depth greater than the equilibrium temperature of the atoms? Figure 22 shows both the Doppler-cooling temperature (eq. (7)) and the dipole potential (eq. (34)) for several intensities. The temperature is always substantially larger than the potential, so such a trap is unstable. This is only one of the issues which needs to be addressed in making a stable dipole trap.

Although the use of the dipole force to trap atoms was first proposed [57] in 1968, the first dipole trap [60] was not realized until 1986. One problem was the inherent instability, discussed above, arising because with a single frequency the temperature will be greater than the well depth. Other problems also contribute to the instability. The issues involved in stabilizing an optical dipole trap can be discussed in connection with the hybrid optical trap proposed by ASHKIN [41] and realized at NIST [61]. The basic laser configuration is the same as that shown in fig. 13. As in that case, the radiation pressure force provides trapping along the laser propagation axis, but now we use the dipole force to stabilize the trap against the radiation pressure force which would expel atoms displaced perpendicularly to the propagation axis. A similar problem involving radiation pressure arises in the Bell Labs single-focus trap [60]. There the radiation pressure tended to force the atoms out along the axis, but with a sufficiently tight focus and a large detuning the dipole force could be made larger than the destabilizing radiation pressure. In the hybrid trap the problem is eas-

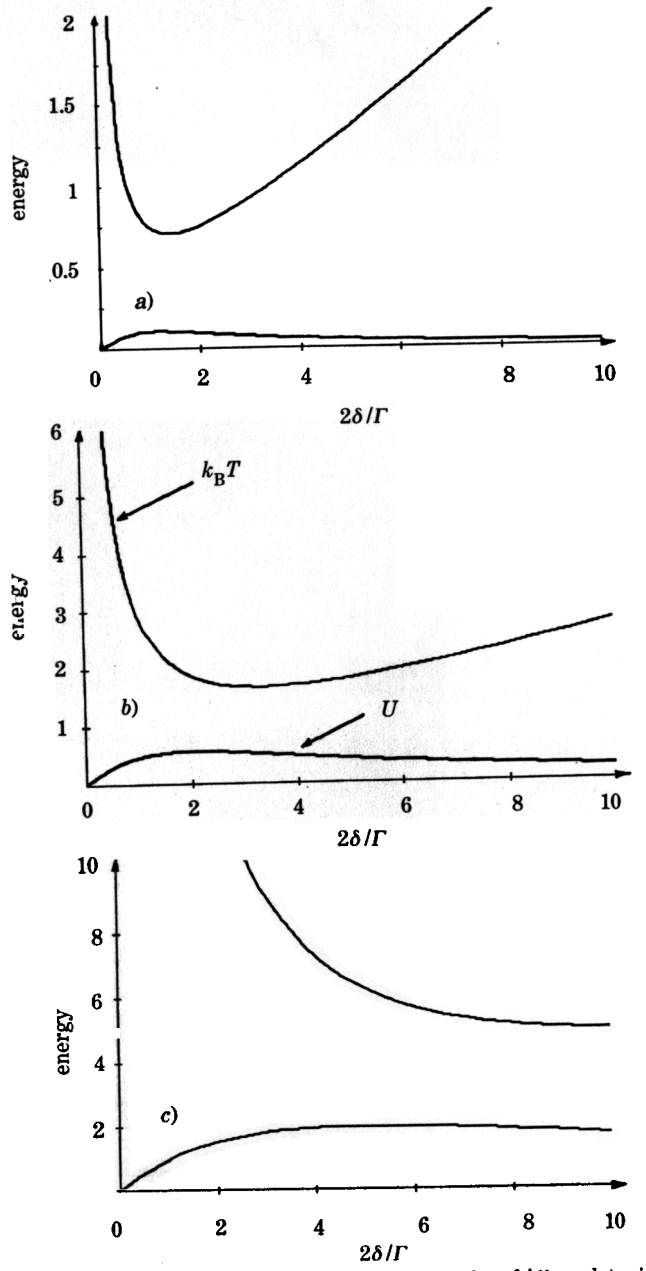

Fig. 22. – Thermal energy k_BT and dipole potential in units of $\hbar\Gamma'$ *vs.* detuning at various intensities: *a*) $I/I_0 = 1$, *b*) $I/I_0 = 10$, *c*) $I/I_0 = 100$.

ier because with the opposed laser beams the radiation pressure force is zero at the same place the dipole force is zero.

We still face the problem that whatever the detuning or intensity the Doppler-cooling temperature is larger than the well depth. A solution, proposed by ASHKIN and GORDON [62], is to use a separate laser beam to cool. Thus the cooling beam could be weak and tuned close to resonance so as to produce a low temperature, while the trap is strong and tuned far from resonance for a large depth. Unfortunately, the same interaction that produces the trapping potential shifts the resonance frequency of the atom, making the cooling less effective. A straightforward solution was proposed by DALIBARD, REYNAUD and COHEN-TANNOUDJI [63]: The trapping and cooling functions are alternated in time. The trapping laser beam is on only half the time, and, while it is off, the cooling can proceed without interference from the trapping beam. This scheme was used by the Bell Labs group to achieve their dipole trap [60].

For the 2-focus trap of fig. 13, there is still another problem. With two opposed beams there is a standing wave, and a strong dipole potential with a periodicity on a wavelength scale. The fluctuations in this dipole force produce a strong heating which can keep the temperature higher than the well depth. This dipole force heating is discussed, for example, in ref. [1, 11-13, 58]. It can be understood as arising from the momentum imparted to an atom by successive cycles of absorption followed by stimulated emission. In a strong standing wave the absorption and stimulated emission can be induced by opposed beams so that a large, but random amount of momentum can be imparted to an atom before a spontaneous emission occurs. The heating which results does not saturate as the intensity increases, but grows without bound. Another way to understand this problem is in the dressed-atom picture [58]. Consider an atom on a given spatially dependent dressed-state potential such as pictured in fig. 20. When the atom undergoes a spontaneous emission, it may decay to the dressed state with the other character, experiencing a reversal of the force (the slope of the potential). Of course, if the atom were to stay at one location, it would, over the course of many such decays, experience an average force equal to the population weighted average of the two dressed-state forces at that location. But this average force has large fluctuations, with the fluctuations becoming larger as the Raby frequency grows. The fluctuations are responsible for the heating or diffusion of momentum arising from the dipole force. This picture for the fluctuation of the dipole force is also useful in understanding the momentum diffusion associated with Sisyphus-type cooling as discussed by COHEN-TANNOUDJI in his lecture at this Summer School.

The solution to the problem of rapid dipole heating in a standing wave is to avoid the standing wave [63]. The two opposed beams are alternated in time so that there is never a standing wave, but the average effect is a trapping potential about half as large as if both beams were on all the time. This technique was used in ref. [61]. The time for alternation here, and in the alternation between

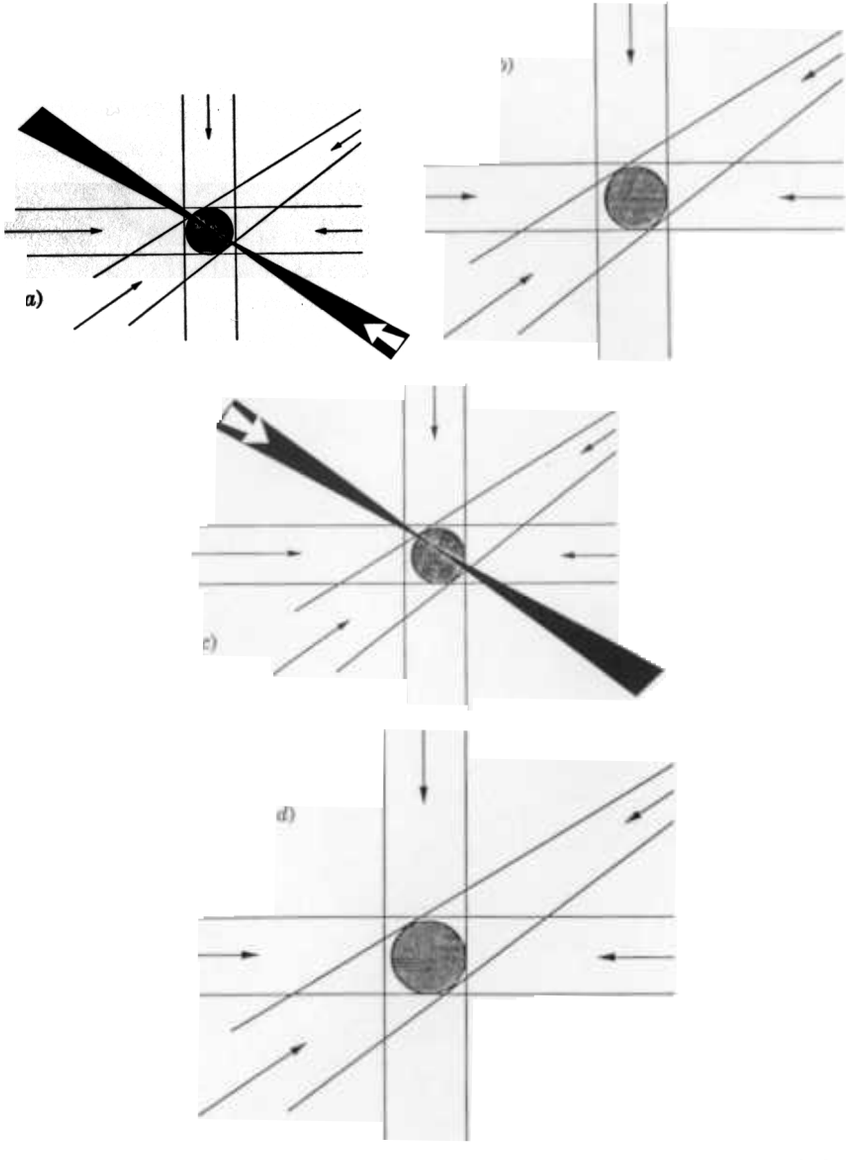

Fig. 23. – Four-phase operation of the two-focus trap: *a*) cycle 1, 1st trap beam; *b*) cycle 2, molasses cooling; *c*) cycle 3, 2nd trap beam; *d*) cycle 4, molasses cooling. Trapping by one focussed laser beam is alternated with cooling and with trapping from the other focussed beam to avoid dipole heating and to retain the effectiveness of cooling in spite of light shifts due to the trapping beams.

cooling and trapping, should be chosen so that it is long compared to the natural lifetime of the excited state, but short compared to the time for oscillation in the trap. In general this is not difficult to achieve, the atomic linewidth being typically some megahertz, while the oscillation frequency is some kilohertz or tens of kilohertz.

A final trick that aids the operation of either a single- or two-focus trap is to load the trap from optical molasses [60]. The trap is embedded in a region of optical molasses filled with cold atoms. This provides a dense source of cold atoms which can fall into the trap. It also provides the cooling, alternated with trapping, that keeps the atom temperature below the well depth.

The time sequence for accomplishing all of this in the two-focus trap at NIST [61] is shown in fig. 23. There are four phases to the alternation of the beams in the trap, with trapping by one focussed beam alternated with molasses, then with the other focussed beam and then with molasses again. In practice the molasses beams are not turned off during the trapping phases because they do not interfere with the trapping.

10·3. *Far off-resonance trap.* – Before discussing an application of trapped atoms, let us consider a proposed modification of the single-focus trap. Recall that in that trap the instability caused by the radiation pressure force pushing atoms axially out of the trap was remedied by detuning the trap from resonance so as to reduce that force, while tightly focussing the laser beam so as to maximize the competing dipole force [60]. Cooling was provided by a separate set of molasses laser beams, and the trapping beam was switched on and off, to allow some periods of cooling free of the large a.c. Stark shifts caused by the trapping laser.

The discovery of cooling below the Doppler-cooling limit has provided the opportunity for new ways of dealing with the problems of dipole trapping. Recall that with polarization gradient cooling or other sub-Doppler-cooling mechanisms the kinetic energy of the atoms is reduced well below the energy $\hbar\Gamma'$ corresponding to the width of the transition. Furthermore, the detuning of the cooling laser is at least several times Γ', in contrast to the case for Doppler cooling where the optimum detuning is about $\Gamma'/2$. Thus a trap whose depth is on the order of or less than $\hbar\Gamma'$ can easily confine such atoms. Furthermore, the a.c. Stark shift induced on the cooling transition by such a trap will be considerably less than the detuning of the cooling laser, so the cooling will not be significantly impaired. This implies that a proper choice of parameters will allow the dipole trap to confine atoms being cooled in molasses without the need for switching the trap on and off. This would allow the full trapping potential to operate, and the full cooling as well, compared to each only acting half the time in the situation requiring switching of the trapping laser.

Since the trap does not need to be very deep to confine the ultra-cold atoms, one can easily tune the trap far from resonance, providing good stability against

the axial radiation pressure force. This has the added advantage of reducing the heating due to the trap laser because the rate of spontaneous emissions is reduced. This rate may be reduced so much that in the absence of the cooling laser beams there is hardly any spontaneous emission and hardly any heating [64]. Such a trap could then hold atoms, mainly in their ground state, for a long time before they were heated enough to escape from the trap.

Referring to fig. 20, a far off-resonance trap (FORT) will have dressed levels that are predominantly either ground- or excited-state character, with little mixing. Trapping is achieved for tuning below resonance and the trap depth is essentially the depth of the ground-state-character dressed potential. This depth is given by $2U/\hbar = (\delta^2 + \Omega^2)^{1/2} - \delta$ which for $\delta \gg \Omega$ gives $U = \hbar\Omega^2/4\delta$. This latter expression is, of course, the light shift of the ground state in this limit. If we choose this trap depth $U \simeq \hbar\Gamma'$, the photon scattering rate will be on the order of Γ'^2/δ. The heating rate is about this scattering rate times the recoil energy. For such a choice of trap depth, the heating due to the trap will be reduced from the saturated rate of spontaneous heating by a factor of Γ'/δ.

As a specific numerical example, consider a trap for Na atoms, where the resonance wavelength is 589 nm, operating off resonance at 750 nm. The detuning is $\delta/2\pi = 10^{14}$ Hz. Since $\Gamma'/2\pi = 10^7$ Hz, $\Gamma'/\delta = 10^{-7}$. For Na, $\Omega = \Gamma'$ at a laser intensity of $12\,\mathrm{mW/cm^2}$, so focussing a 2 W Gaussian beam to a 14 μm radius gives $\Omega/\Gamma' = 7 \cdot 10^3$ at the center. This leads to a well depth about equal to $\hbar\Gamma'$, and a photon scattering rate less than $10\,\mathrm{s^{-1}}$. The rate of increase of the atomic temperature, in the absence of cooling (remembering that the energy increases on average by a recoil energy for both emission and absorption, that the recoil is for a 750 nm photon and that the energy is distributed in three dimensions by the trapping forces), is less than $10\,\mu\mathrm{K\,s^{-1}}$. Thus, since $\hbar\Gamma'/k_B \simeq 500\,\mu\mathrm{K}$, the atoms will take several tens of seconds to boil out of the trap, even with no cooling. It may be possible to hold high densities of ground-state atoms in such a trap for long enough to observe quantum collective effects.

A first step toward the realization of such a trap has recently been made at NIST, where HELMERSON and colleagues [65] observed trapping of Na about 5 nm off resonance, a condition which permitted continuous rather than switched operation of the trap, with continuous cooling by optical molasses.

11. – Collision experiments in optical traps.

The lecture of JULIENNE at this Summer School covers the theory of collisions between cold atoms. Here we will briefly describe just one set of experiments which observe collisions between laser-cooled and trapped Na atoms at NIST. The trap used is the hybrid two-focus trap described above in subsect. 10·2. The collision observed is known as associative ionization and may be

written

$$\text{Na} + \text{Na} + 2h\nu \rightarrow \text{Na}_2^+ + \text{e}^- \ . \tag{35}$$

At higher energies it is thought of as being a collision between two excited ($3P$) Na atoms in which the energy of excitation is given up to ionize the electron, with the binding energy of the molecule supplying some of the needed energy. The reaction is experimentally convenient because an ion can be easily detected and because a process such as Penning ionization (energy transfer and ionization without formation of a molecule) is not energetically allowed.

The experiments are described in ref. [61, 66]. The sodium atoms were collected in the optical trap where they achieved densities on the order of $10^{10}\,\text{cm}^{-3}$ in a volume of about $10^{-6}\,\text{cm}^3$. The atomic temperature was less than about 1 mK, and the trap depth was about 10 mK. The production rate of ions R_{ion} was measured with an electron multiplier that simply pulled the ions out of the trap and counted them. At the same time, the excited-state population and distribution of atoms was determined by photographing the trapped atoms with a high-resolution, calibrated video camera. From these data we determined the «cross-section» σ_{AI} for associative ionization defined according to

$$R_{\text{ion}} = n_{\text{ex}}\,\sigma_{\text{AI}}\,\langle v\rangle\,N_{\text{ex}} \ , \tag{36}$$

where n_{ex} is the excited-state density appropriately averaged over the confinement volume of the trap, N_{ex} is the total number of excited atoms and $\langle v\rangle$ is the average collision velocity. We found [61] this cross-section to be about $10^{-13}\,\text{cm}^2$, which is three orders of magnitude higher than the cross-section at any higher temperature measured at that time. This large increase in cross-section illustrates the interesting nature of collision processes at low energy.

At these low energies, however, the concept of cross-section is not a very good one. The idea of a cross-section, as implied by eq. (36), assumes that collision partners are prepared in a certain way prior to the collisions, they collide and form products which are observed. In fact, these collisions occur so slowly because of the low kinetic energy of the reactants, that the state of the atoms undergoes continuous evolution during the collision. The observation of a certain density of excited atoms in the trap does not mean that that many excited atoms are available to undergo an associative ionization collision. By the time two atoms get close enough together to form a molecule, the energy shifts associated with the atom-atom interaction will have shifted the atoms' internal energy levels out of resonance with the laser, and the atoms may have decayed to the ground state. JULIENNE predicted that this phenomenon would result in an ion production rate that depended strongly on laser intensity. That is, ions should be formed mainly during those periods when the trap laser is on (recall that the trap laser must be switched on and off to allow the cooling lasers to work effectively). Exactly that behavior was observed in ref. [66], in agreement with the prediction of Julienne [67].

12. – Emission spectrum of laser-cooled atoms.

In his 1968 paper [57] LETOKHOV suggested trapping atoms in the intensity gradients of a standing-wave light field. Such atoms, confined to a spatial region smaller than a wavelength of light, would exhibit a suppression of the Doppler broadening of their spectrum (Dicke narrowing). An experiment demonstrating this effect was recently performed at NIST [68].

The experiment measures the emission spectrum of atoms being laser cooled in optical molasses. Stationary atoms irradiated with a single laser frequency at low intensity emit spontaneous photons at that same frequency, as can be understood by energy conservation. If the atoms are moving, the emitted light is Doppler shifted from the irradiating frequency, again an effect of conservation of energy and momentum. For higher-intensity illumination, the radiated spectrum for stationary atoms is the fluorescent (Mollow) triplet plus a component at the laser frequency [69]. This latter component is sometimes called the elastic or coherent part of the emission spectrum. It is subject to Doppler broadening, just as for low intensity, and otherwise it will be as broad as the incident laser frequency.

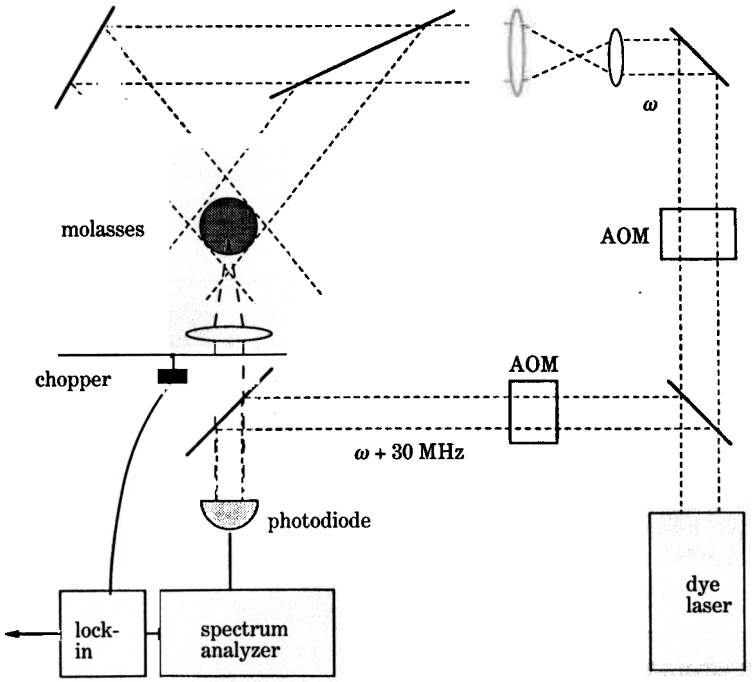

Fig. 24. – Schematic representation of the apparatus for a heterodyne measurement of the spectrum of light emitted by atoms in optical molasses.

The experimental setup for observing this Doppler-broadened elastic line is shown in fig. 24. The fluorescence from the optical molasses is collected with a lens and combined with a reference beam, derived from the molasses laser, on a photodiode. Using acousto-optic modulators the reference beam is shifted by about 30 MHz from the frequency which illuminates the molasses. This means that the beat frequency between the fluorescence and the reference will be centered around 30 MHz. Use of this high frequency avoids problems with laser noise occurring at lower frequencies. The heterodyne beat signal is processed using a radiofrequency spectrum analyzer, which displays the power spectrum of the current from the photodiode. It can be shown [70] that this r.f. spectrum corresponds to the optical power spectrum emitted by the atoms. The lock-in amplifier, synchronized with the chopping of the fluorescence, serves to reduce some low-frequency noise but does not alter the spectrum. Frequency fluctuations of the molasses laser are not recorded as part of the heterodyne spectrum, even though they are in the optical power spectrum, because the reference laser has identical fluctuations, so these fluctuations do not appear in the beat frequency.

Because the bandwidth of the r.f. spectrum analyzer is quite narrow (typically tens of kilohertz) the spectral density of the broad (order of 10 MHz) Mol-

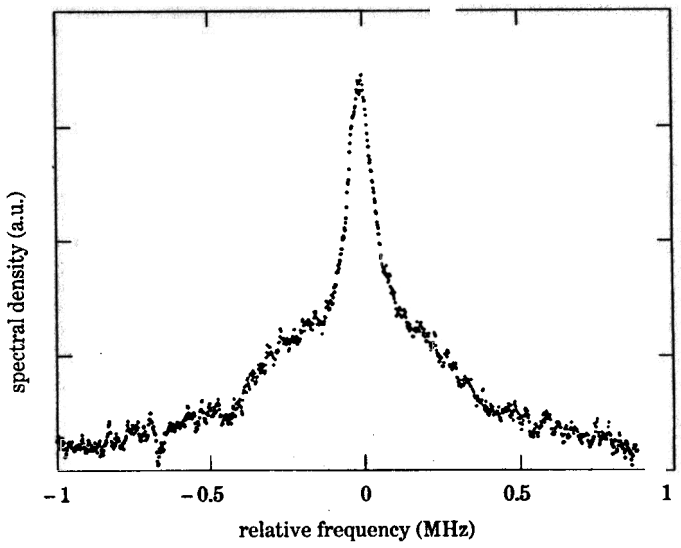

Fig. 25. – Typical spectrum of fluorescent light from optical molassess with a laser detuning from resonance of -2Γ. The narrow feature indicates Dicke narrowing due to confinement of atoms in standing-wave potential wells.

low spectrum is so small that it is negligible in this experiment. The elastic component, however, is Doppler broadened to less than 1 MHz and appears clearly. An example of such a spectrum is shown in fig. 25. The broad component is the Doppler-broadened elastically scattered light. The breadth corresponds to a temperature of about 70 μK, in agreement with the temperature measured by a time-of-flight technique for atoms illuminated at the same intensity and detuning. A striking feature of the spectrum is the sharp peak, centered on the Doppler peak, having a width of only 70 kHz. This narrowed peak was interpreted as arising from the confinement of atoms in the standing waves produced by the interference of the molasses laser beams.

This Dicke narrowing [71] can be understood in the context of phase modulation of the emitted light. Consider a stationary atom illuminated by a fixed frequency and radiating that same frequency. If the position of the atom changes, its distance from the source and to the observer changes, so the phase of the emitted light seen by the observer is shifted. For an oscillating atom there is a periodic modulation of the phase, and the spectrum of the emitted light acquires sidebands spaced at the modulation frequency. The amount of the phase modulation, or the modulation index, is determined by the amplitude of the atomic motion, the phase shift being $\Delta x \cdot \Delta k$, where Δx is the displacement of the atom and Δk is the difference in wave vectors of the absorbed and emitted light. When the amplitude of this modulated phase shift is large compared to unity, there are many sidebands in the spectrum and little power is radiated at the incident or carrier frequency. But when the atom's motion is confined to less than a wavelength of light, the phase modulation is small and much of the power is still radiated at the carrier frequency. In the limit that the atom is confined to much less than a wavelength, all of the power is radiated in the carrier, regardless of the frequency of the modulation. Thus the atoms, trapped in the microscopic potential wells of the standing waves in optical molasses, radiate a spectrum having a component free of Doppler broadening. The breadth of this narrow component reflects the finite confinement time, and the Doppler-broadened component represents unconfined movement of atoms as well as the unresolved sidebands radiated by trapped atoms.

While this experiment gave the first observation of Dicke narrowing due to confinement of atoms in wavelength-scale optical potentials, earlier work at ENS demonstrated 1-D confinement, or channeling of atoms in such an optical potential [72]. In that experiment the atoms were channeled through a strong, 1-D standing wave. The atomic motion was nearly Hamiltonian in the sense that dissipative processes were not important over the time the channeling occurred. By contrast, in the 3-D experiment described above, the atoms were in equilibrium with the cooling and heating forces.

In considering experiments such as the one described above, it is important to remember that such a heterodyne measurement of the spectrum is a true measurement of the power spectrum of the emitted light and that it is not a

phase-sensitive measurement. The fact that the experiment is particularly sensitive to the «coherent» part of the radiated spectrum has nothing to do with the fact that the coherent part of the fluorescence is phase coherent with the laser. In fact, that phase coherence only holds for a single atom at rest. In our experiment the various atoms in the molasses all radiate coherent components with different and time-varying phases. These add incoherently to produce the observed spectrum. The heterodyne technique is certainly also capable of seeing the «incoherent» or Mollow spectrum, but the greater breadth of that spectrum makes it harder to see. Preliminary measurements at NIST using a more efficient processing of the heterodyne signal may have already seen evidence of the central Mollow component in the heterodyne spectrum [73].

* * *

I give my very sincere thanks to all my colleagues at NIST: staff, postdocs, students and visitors, who have contributed so much to the understanding of laser cooling and trapping and to the advancement of its practice and application. I am also indebted to my colleagues at the Ecole Normale Supérieure, Paris, for their hospitality and instruction during the academic year of 1989-1990 when I was a visitor in their laboratory.

These lecture notes have not been in any sense a review of the vast amount of experimental and theoretical work in laser cooling and trapping of neutral atoms. My neglect of so many important experiments and theoretical treatments has been mandated by space limitations and pedagogical considerations; I gratefully acknowledge the contributions of colleagues all over the world, both cited and not, who have made the study of laser cooling and trapping such a rewarding experience.

I thank the National Institute of Standards and Technology and the Office of Naval Research for their crucial financial and moral support of work on laser cooling and trapping at NIST.

REFERENCES

[1] *Fundamental Systems in Quantum Optics*, Les Houches, Session LII, 1990, edited by J. DALIBARD, J. M. RAIMOND and J. ZINN-JUSTIN (Elsevier Science Publishers B. V., Amsterdam, 1992), to be published (see in particular the notes of C. COHEN-TANNOUDJI, H. WALTHER, R. BLATT and W. PHILLIPS).

[2] S. V. ANDREEV, V. I. BALYKIN, V. V. LETOKHOV and V. G. MINOGIN: *JETP Lett.*, **34**, 442 (1981).

[3] W. D. PHILLIPS, J. PRODAN and H. METCALF: *J. Opt. Soc. Am. B*, **2**, 1751 (1985).

[4] W. D. PHILLIPS and H. J. METCALF: *Phys. Rev. Lett.*, **49**, 1149 (1982).

[5] M. ZHU, C. W. OATES and J. L. HALL: *Phys. Rev. Lett.*, **67**, 46 (1991), and references therein.

[6] W. KETTERLE, A. MARTIN, M. A. JOFFE and D. E. PRITCHARD: to be published; see also J. UMEZU and F. SHIMIZU: *Jpn. J. Appl. Phys.*, **24**, 1655 (1985), and the lecture of PRITCHARD and KETTERLE at this Summer School.

[7] V. S. LETOKHOV, V. G. MINOGIN and B. D. PAVLIK: *Opt. Commun.*, **19**, 72 (1976).

[8] W. D. PHILLIPS and J. PRODAN: in *Laser Cooled and Trapped Atoms*, edited by W. PHILLIPS, *Natl. Bur. Stand. (U.S.) Spec. Publ.* **653**, 137 (1983); *Prog. Quantum Electron.*, **8**, 231 (1984); in *Coherence and Quantum Optics V*, edited by L. MANDEL and E. WOLF (Plenum, New York, N.Y., 1984), p. 15; W. PHILLIPS, J. PRODAN and H. METCALF: in *Laser Spectroscopy VI*, edited by H. WEBER and W. LUTHY (Springer-Verlag, Berlin, 1983), p. 162.

[9] W. ERTMER, R. BLATT and J. HALL: *Phys. Rev. Lett.*, **54**, 996 (1985).

[10] C. SALOMON and J. DALIBARD: *C. R. Acad. Sci. Paris*, **306**, 1319 (1988).

[11] *a*) J. GORDON and A. ASHKIN: *Phys. Rev. A*, **21**, 1606 (1980); *b*) R. COOK: *Phys. Rev. A*, **22**, 1078 (1980); *c*) S. STENHOLM: *Rev. Mod. Phys.*, **58**, 699 (1986).

[12] J. DALIBARD: Thèse de doctorat d'état es Sciences Physiques (Université de Paris, Paris, 1986).

[13] C. COHEN TANNOUDJI: in *Fundamental Systems in Quantum Optics*, Les Houches, Session LII, 1990, edited by J. DALIBARD, J. M. RAIMOND and J. ZINN-JUSTIN (Elsevier Science Publishers B. V., Amsterdam, 1992), to be published.

[14] J. JAVANAINEN, M. KAIVOLA, U. NIELSEN, O. POULSEN and E. RIIS: *J. Opt. Soc. Am. B*, **2**, 1768 (1985).

[15] S. CHU, L. HOLLBERG, J. BJORKHOLM, A. CABLE and A. ASHKIN: *Phys. Rev. Lett.*, **55**, 48 (1985).

[16] T. HÄNSCH and A. SCHAWLOW: *Opt. Commun.*, **13**, 68 (1975).

[17] D. WINELAND and H. DEHMELT: *Bull. Am. Phys. Soc.*, **20**, 637 (1975).

[18] J. DALIBARD, S. REYNAUD and C. COHEN-TANNOUDJI: *J. Phys. B*, **17**, 4577 (1984).

[19] P. LETT, W. PHILLIPS, S. ROLSTON, C. TANNER, R. WATTS and C. WESTBROOK: *J. Opt. Soc. Am. B*, **6**, 2084 (1989).

[20] D. SESKO, C. FAN and C. WIEMAN: *J. Opt. Soc. Am. B*, **5**, 1225 (1988).

[21] S. CHU, M. PRENTISS, A. CABLE and J. BJORKHOLM: in *Laser Spectroscopy VIII*, edited by W. PERSSON and S. SVANBERG (Springer-Verlag, Berlin, 1987), p. 58.

[22] P. GOULD, P. LETT and W. PHILLIPS: in *Laser Spectroscopy VIII*, edited by W. PERSSON and S. SVANBERG (Springer-Verlag, Berlin, 1987), p. 64.

[23] P. LETT, R. WATTS, C. WESTBROOK, W. PHILLIPS, P. GOULD and H. METCALF: *Phys. Rev. Lett.*, **61**, 169 (1988).

[24] W. PHILLIPS, C. WESTBROOK, P. LETT, R. WATTS, P. GOULD and H. METCALF: in *Atomic Physics 11*, edited by S. HAROCHE, J. GAY and G. GRYNBERG (World Scientific, Singapore, 1989), p. 633.

[25] J. DALIBARD and C. COHEN-TANNOUDJI: *J. Opt. Soc. Am. B*, **6**, 2023 (1989).

[26] P. UNGAR, D. WEISS, E. RIIS and S. CHU: *J. Opt. Soc. Am. B*, **6**, 2058 (1989).

[27] J. DALIBARD, C. SALOMON, A. ASPECT, E. ARIMONDO, R. KAISER, N. VANSTEENKISTE and C. COHEN-TANNOUDJI: in *Atomic Physics 11*, edited by S. HAROCHE, J. C. GAY and G. GRYNBERG (World Scientific, Singapore, 1989), p. 199.

[28] D. S. WEISS, E. RIIS, Y. SHEVY, P. J. UNGAR and S. CHU: *J. Opt. Soc. Am. B*, **6**, 2072 (1989).

[29] B. SHEEHY, S.-Q. SHANG, P. VAN DER STRATEN, S. HATAMIAN and H. METCALF: *Phys. Rev. Lett.*, **64**, 858 (1990); S.-Q. SHANG, B. SHEEHY, P. VAN DER STRATEN and H. METCALF: *Phys. Rev. Lett.*, **65**, 317 (1990); S.-Q. SHANG, B. SHEEHY,

H. METCALF, P. VAN DER STRATEN and G. NIENHUIS: *Phys. Rev. Lett.*, **67**, 1094 (1991).
[30] Y. CASTIN, J. DALIBARD and C. COHEN-TANNOUDJI: in *Light Induced Kinetic Effects on Atoms, Molecules and Ions*, edited by L. MOI, S. GOZZINI, C. GABBIANI, E. ARIMONDO and F. STRUMIA (ETS Editrice, Pisa, 1991), p. 5.
[31] C. SALOMON, J. DALIBARD, W. PHILLIPS, A. CLAIRON and S. GUELLATI: *Europhys. Lett.*, **12**, 683 (1990).
[32] The idea of an atomic-fountain clock, originated by ZACHARIAS, is described in N. F. RAMSEY: *Molecular Beams* (Oxford University Press, Oxford, 1985), p. 138, 285.
[33] S. L. ROLSTON and W. D. PHILLIPS: *Proc. IEEE*, **79**, 943 (1991).
[34] M. KASEVICH, E. RIIS, R. DEVOE and S. CHU: *Phys. Rev. Lett.*, **63**, 612 (1989).
[35] A. CLAIRON, C. SALOMON, S. GUELLATI and W. PHILLIPS: *Europhys. Lett.*, **16**, 165 (1991).
[36] K.-J. KÜGLER, W. PAUL and U. TRINKS: *Phys. Lett. B*, **72**, 422 (1978); C. V. HEER: *Rev. Sci. Instrum.*, **34**, 532 (1963); see also V. V. VLADIMIRSKII: *Sov. Phys. JETP*, **12**, 740 (1961).
[37] A. MIGDALL, J. PRODAN, W. PHILLIPS, T. BERGEMAN and H. METCALF: *Phys. Rev. Lett.*, **54**, 2596 (1985).
[38] V. BAGNATO, G. LAFYATIS, A. MARTIN, E. RAAB, R. AHMAD-BITAR and D. PRITCHARD: *Phys. Rev. Lett.*, **58**, 2194 (1987); A. MARTIN, K. HELMERSON, V. BAGNATO, G. LAFYATIS and D. PRITCHARD: *Phys. Rev. Lett.*, **61**, 2431 (1988).
[39] H. HESS, G. KOCHANSKI, J. DOYLE, N. MASHUHARA, D. KLEPPNER and T. GREYTAK: *Phys. Rev. Lett.*, **59**, 672 (1987); R. VAN ROIJEN, J. BERHOUT, S. JAAKKOLA and J. WALRAVEN: *Phys. Rev. Lett.*, **61**, 931 (1988).
[40] E. CORNELL, C. MONROE and C. WIEMAN: *Phys. Rev. Lett.*, **67**, 2439 (1991).
[41] A. ASHKIN: *Phys. Rev. Lett.*, **40**, 729 (1978).
[42] V. BALYKIN, V. LETOKHOV and A. SIDOROV: *Pis'ma Ž. Èksp. Teor. Fiz.*, **43**, 172 (1986).
[43] V. BALYKIN and V. LETOKHOV: *Physics Today*, April 1989, p. 23.
[44] A. ASHKIN and J. GORDON: *Opt. Lett.*, **8**, 511 (1983).
[45] A. ASHKIN: *Opt. Lett.*, **9**, 454 (1984).
[46] J. DALIBARD and W. PHILLIPS: *Bull. Am. Phys. Soc.*, **30**, 748 (1985).
[47] D. PRITCHARD, E. RAAB, V. BAGNATO, C. WIEMAN and R. WATTS: *Phys. Rev. Lett.*, **57**, 310 (1986).
[48] See the closing remarks in ref. [49].
[49] E. RAAB, M. PRENTISS, A. CABLE, S. CHU and D. PRITCHARD: *Phys. Rev. Lett.*, **59**, 2631 (1987).
[50] A. STEANE and C. FOOT: *Europhys. Lett.*, **14**, 231 (1991).
[51] F. SHIMIZU, K. SHIMIZU and H. TAKUMA: *Chem. Phys.*, **145**, 327 (1990).
[52] A. CABLE, M. PRENTISS and N. P. BIGELOW: *Opt. Lett.*, **15**, 507 (1990); C. MONROE, S. SWANN, H. ROBINSON and C. WIEMAN: *Phys. Rev. Lett.*, **65**, 1571 (1990).
[53] M. PRENTISS, A. CABLE, J. BJORKHOLM, S. CHU, E. RAAB and D. PRITCHARD: *Opt. Lett.*, **13**, 452 (1988); D. SESKO, T. WALKER, C. MONROE, A. GALLAGHER and C. WIEMAN: *Phys. Rev. Lett.*, **63**, 961 (1989).
[54] T. WALKER, D. SESKO and C. WIEMAN: *Phys. Rev. Lett.*, **64**, 408 (1990).
[55] E. RIIS, D. WEISS, K. MOLER and S. CHU: *Phys. Rev. Lett.*, **64**, 1658 (1990).
[56] J. NELLESSEN, J. WERNER and W. ERTMER: *Opt. Commun.*, **78**, 300 (1990).
[57] V. S. LETOKHOV: *JETP Lett.*, **7**, 272 (1968).
[58] J. DALIBARD and C. COHEN-TANNOUDJI: *J. Opt. Soc. Am. B*, **2**, 1707 (1985).

[59] C. AGOSTA, I. SILVERA, H. STOOF and B. VERHAAR: *Phys. Rev. Lett.*, **62**, 2361 (1989).
[60] S. CHU, J. BJORKHOLM, A. ASHKIN and A. CABLE: *Phys. Rev. Lett.*, **57**, 314 (1986).
[61] P. GOULD, P. LETT, P. JULIENNE, W. PHILLIPS, H. THORSHEIM and J. WEINER: *Phys. Rev. Lett.*, **60**, 788 (1988).
[62] A. ASHKIN and J. GORDON: *Opt. Lett.*, **4**, 161 (1979).
[63] J. DALIBARD, S. REYNAUD and C. COHEN-TANNOUDJI: *Opt. Commun.*, **47**, 395 (1983); *J. Phys. B*, **17**, 4577 (1984), and private communications.
[64] S. CHU, J. BJORKHOLM, A. ASHKIN, J. GORDON and L. HOLLBERG: *Opt. Lett.*, **11**, 73 (1986).
[65] K. HELMERSON: presented at the *Interdisciplinary Laser Conference, Monterey, California, September 1991* (unpublished).
[66] P. LETT, W. PHILLIPS, S. ROLSTON, C. WESTBROOK and P. GOULD: *Phys. Rev. Lett.*, **76**, 2139 (1991).
[67] P. JULIENNE: *Phys. Rev. Lett.*, **61**, 698 (1988); P. JULIENNE and R. HEATHER: *Phys. Rev. Lett.*, **67**, 2135 (1991).
[68] C. WESTBROOK, R. WATTS, C. TANNER, S. ROLSTON, W. PHILLIPS and P. LETT: *Phys. Rev. Lett.*, **65**, 33 (1990).
[69] B. MOLLOW: *Phys. Rev.*, 188, 1969 (1969).
[70] See, for example, L. DRAIN: *The Laser Doppler Technique* (Wiley, New York, N.Y., 1980).
[71] R. DICKE: *Phys. Rev.*, **89**, 472 (1953).
[72] C. SALOMON, J. DALIBARD, A. ASPECT, H. METCALF and C. COHEN-TANNOUDJI: *Phys. Rev. Lett.*, **59**, 1659 (1987).
[73] C. WESTBROOK, P. JESSEN, C. TANNER, P. LETT, S. ROLSTON, R. WATTS and W. PHILLIPS: in *Atomic Physics 12*, edited by J. ZORN and R. LEWIS (American Institute of Physics, New York, N.Y., 1991), p. 89.

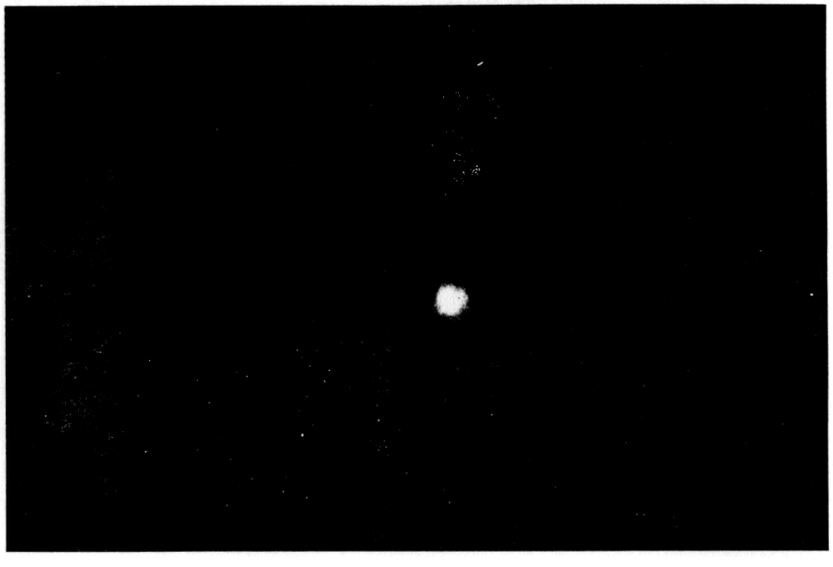

Plate II. – Optical molasses for sodium atoms is seen as a bright area at the intersection of three pairs of centimeter diameter, counterpropagating laser beams. The additional laser beam above the molasses decelerates the atomic sodium beam so the atoms are slow enough to be captured by the molasses (photo courtesy of NIST).

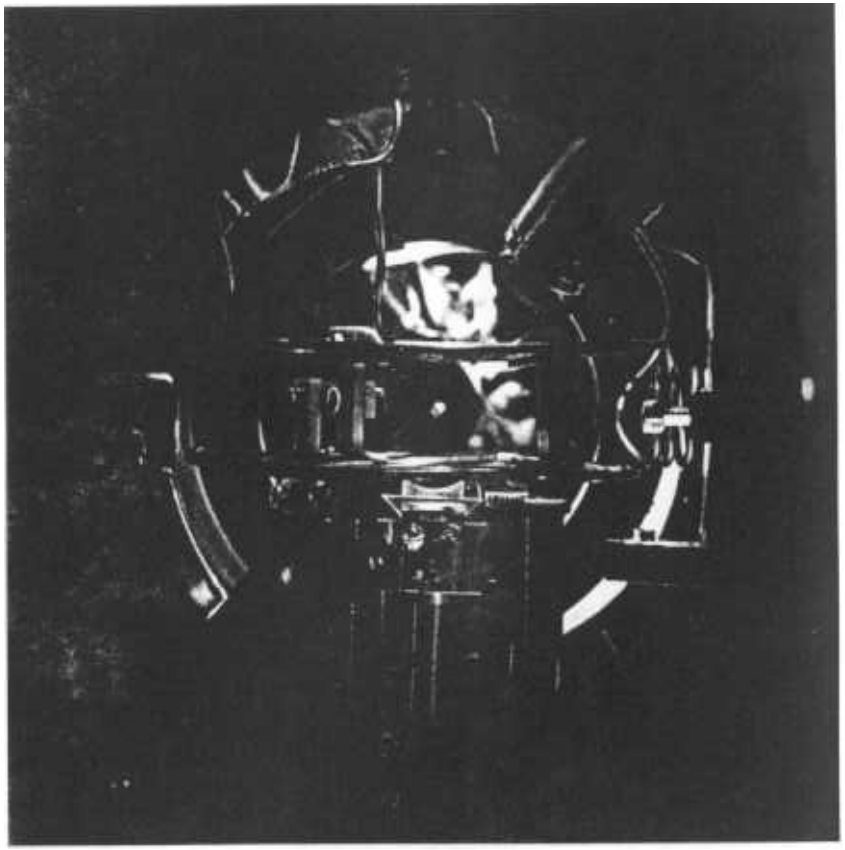

Plate III. – Sodium atoms held in a magneto-optical trap (MOT) appear as a bright, millimeter-size spot between the pair of flat coils which produce the magnetic-field gradient. Fluorescence from the centimeter diameter laser beam pairs forming the MOT is too weak to be visible in the photograph (photo by M. HELFER, courtesy of NIST).